

Online recognition of the multiphase flow regime and study of slug flow in pipeline

GUO Liejin¹, BAI Bofeng¹, ZHAO Liang¹, Wang Xin¹, Gu Hanyang¹

¹ Xi'an Jiaotong University, Xi'an 710049, CHINA

lj-guo@mail.xjtu.edu.cn

Abstract. Multiphase flow is the phenomenon existing widely in nature, daily life, as well as petroleum and chemical engineering industrial fields. The interface structure among multiphase and their movement are complicated, which distribute random and heterogeneously in the spatial and temporal scales and have multivalued flow structure and state^[1]. Flow regime is defined as the macro feature about the multiphase interface structure and its distribution, which is an important feature to describe multiphase flow. The energy and mass transport mechanism differ much for each flow regimes. It is necessary to solve the flow regime recognition to get a clear understanding of the physical phenomena and their mechanism of multiphase flow. And the flow regime is one of the main factors affecting the online measurement accuracy of phase fraction, flow rate and other phase parameters. Therefore, it is of great scientific and technological importance to develop new principles and methods of multiphase flow regime online recognition, and of great industrial background.

In this paper, the key reasons that the present method cannot be used to solve the industrial multiphase flow pattern recognition are clarified firstly. Then the prerequisite to realize the online recognition of multiphase flow regime is analyzed, and the recognition rules for partial flow pattern are obtained based on the massive experimental data. The standard templates for every flow regime feature are calculated with self-organization cluster algorithm. The multi-sensor data fusion method is proposed to realize the online recognition of multiphase flow regime with the pressure and differential pressure signals, which overcomes the severe influence of fluid flow velocity and the oil fraction on the recognition. The online recognition method is tested in the practice, which has less than 10 percent measurement error. The method takes advantages of high confidence, good fault tolerance and less requirement of single sensor performance.

Among various flow patterns of gas-liquid flow, slug flow occurs frequently in the petroleum, chemical, civil and nuclear industries. In the offshore oil and gas field, the maximum slug length and its statistical distribution are very important for the design of separator and downstream processing facility at steady state operations. However transient conditions may be encountered in the production, such as operational upsets, start-up, shut-down, pigging and blowdown, which are key operational and safety issues related to oil field development. So it is necessary to have an understanding the flow parameters under transient conditions. In this paper, the evolution of slug length along a horizontal pipe in gas-liquid flow is also studied in details and then an

experimental study of flowrate transients in slug flow is provided. Also, the special gas-liquid flow phenomena easily encountered in the life span of offshore oil fields, called severe slugging, is studied experimentally and some results are presented.

1. INTRODUCTION

Multiphase flow is a phenomenon which exists widely in petroleum, chemical engineering industrial fields, as well as in natural, life living. The interfacial structure between phases and its movement is very complicated, which has the randomness and heterogeneity distribution in the spatial and temporal scales, therefore, the flow structure and state of multiphase mixture is in multivalued. Flow pattern is defined as the macro feature about the multiphase interfacial structure and their distribution, which is an important feature to describe multiphase flow. When gas and liquid two-phase flow in a pipe, several flow patterns can be observed, including typical stratified and slug flow. The energy and mass transport mechanism differs much for different flow patterns. It is necessary to solve the recognition of flow patterns to get a clear understanding of the physical phenomena and their mechanism of multiphase flow. And the flow regime is one of the main factors affecting the online measurement accuracy of phase fraction, flow rate and other phase parameters. Therefore, it is of great scientific and technological importance to develop new principles and methods of multiphase flow regime online recognition, and of great industrial background as described in Guo (2002, 2005).

The one of the earliest research work with online recognition of flow regime was presented by Hubbard and Dukler (1966), in which they proposed a method based on pressure fluctuation probability density function. Until now, the flow regime recognition methods can be classified into two categories. One is on basis of flow structure image directly, and the other is the indirect method, that is, the recognition with the analysis of fluctuation signal representing the multiphase flow character. The indirect method is becoming main approach because it can quantitatively describe the flow regime. The fluctuating signals about flow regime have many feature extraction methods, such as time series analysis, wavelet, time-frequency joint analysis, fuzzy, chaos and fractal by Tutu 1984; Matsui (1986); Wambsganss & Jendrzeczyk (1991); Cai, Wambsganss & Jendrzeczyk (1996); and Langford, Beasley & Ochterbeck (1998). The artificial neural network has been developed to a conventional method to recognize the flow regime by Mi, Ishii & Tsoukalas (1998); Monji & Matsu (1998); Wu & Zhou (2001); and Mahvash & Ross (2008).

Until now all the online recognition methods proposed in previous publications still could not give a satisfactory solution for the industry flow due to their little reliability and repeatability as pointed out by Bai, Guo & Zhao (2001); Li (2002); Yang et al (2005), and Bai et al (2008). The main reasons are as follows:

- (1) The fluid physical properties and flow velocity have great influence on the recognition accuracy.
- (2) The feature parameter intersects for different flow regime, which make it is unable to identify accurately basing on one single technology.

The physical mechanism resulted in pressure fluctuation can explain the two reasons. The pressure fluctuation is caused by the phase interface movement and its induced turbulence, the bilateral differential pressure, as well the liquid turbulence by Samways, Bradbury & Bruun (1997). The oil-gas-water multiphase flow as the example, its great flow rate and great oil fraction will certainly reduce the sensitivity of the pressure fluctuation to the phase movement and distribution.

In this paper, the prerequisite is analyzed to realize the online recognition of multiphase flow regime firstly. Secondly the recognition rules for partial of flow pattern are discussed and given basing on the feature analysis of pressure signal and differential pressure signal. Then the self-organization cluster algorithm is proposed to design the standard templates for every flow pattern feature. At last, the multi-sensor data fusion method is proposed to recognize the multiphase flow regime, which is tested in the practice.

Among various flow patterns of gas-liquid flow, gas-liquid slug flow occurs frequently in the petroleum, chemical, civil and nuclear industries. It is characterized by a sequence of elongated

bubbles separated by liquid slugs that may contain small bubbles. It can be divided into two main groups: hydrodynamic and terrain slugging. Hydrodynamic slugging is the normal slugging pattern encountered in straight flow lines. Terrain slugging results from variable flow line topography which lead to local dips and peaks in the flow. An extreme case of this form of slugging occurs when a slightly downwardly inclined flow line is connected to a vertical riser which connects the flow line to the platform-mounted separator. Severe slugging often results in large backpressure accumulation, as well as widely varying liquid and gas production levels. For its transient and intermittent nature, it is difficult to predict the flow characteristics correctly. Therefore, reliable flow models are crucial for the safe and cost efficient design and operation of industrial facilities. This paper describes the experimental and numerical investigations on the slug flow in pipeline in our laboratory.

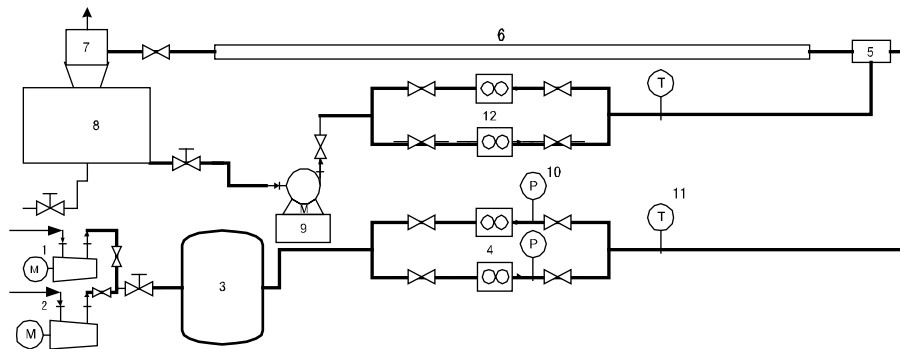


Fig. 1 Schematic of the experimental system

- 1, 2: Air Compressor; 3: Air tank; 4: Air flowmeters; 5: Mixer; 6: Test section; 7: Separator;
 8: Water tank; 9: Centrifugal pump; 10: ROSEMOUNT pressure transducer;
 11: Thermocouple; 12: Liquid flowmeters

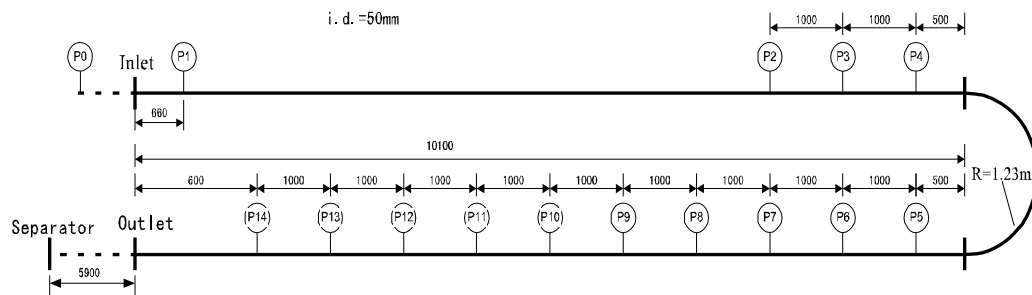


Fig. 2 Measurement instruments on the test section

2. EXPERIMENTAL FACILITY AND MEASUREMENT SYSTEM

The experiments were carried out in a test facility as shown in Fig. 1. The test section is a 27.33m long PVC pipe with internal diameter of 0.05m. There is a U-type elbow ($R=1.23m$) in the middle of the test loop, as shown in Fig. 2. The pipe is supported by a steel frame and can be rotated around its axis. In this study the test section is fixed horizontally. The working fluids are air and water.

Fig. 2 gives the locations of the instruments installed on the test section. There are 14 KELLER PA23e pressure transducers, which are sequenced from P1 to P14 along the tube. The frequency response of the KELLER PA23e pressure transducers is 5kHz, which is high enough to record the transient characteristics of slug flow. The analog output signals from pressure transducers and

flowmeters were sampled by a 12-bit PCI-6071e data acquisition card produced by NATIONAL INSTRUMENTS company running on a personal computer. The sampling frequency of each channel is setting at 2500Hz.

The slug flow parameters in the pipe were detected by the fast response pressure transducers. This method was presented in the Ph.D. dissertation of He (2002). In this paper the signal of pressure transducer was compared with that of the double parallel wire conductivity probes. It is found that the sharp increasing edge of the pressure is corresponding to the front of the liquid slug, as shown in Fig.3, 4. However, when the tail of the liquid slug leaves the pressure transducer there is no clear mark in the pressure signal. But if we subtract the downstream pressure from the upstream pressure we can get the differential pressure and the end of the sharp decreasing edge is corresponding to the moment of the tail of the liquid slug leaving the downstream pressure transducer. The beginning point of the sharp increasing edge of the differential pressure trace is the moment that the liquid slug front arrives at the upstream pressure transducer. Therefore liquid slug translational velocity and its length can be measured from three neighboring pressure transducers. In this study, ten pressure transducers from P5 to P14 were installed on the test section and all the separation distances between two neighboring taps were 1m. Fig.4 shows the differential pressure traces from the subtractions of three close pressure transducer signals. The slug translational velocity is:

$$V_t = \frac{L}{t_1} \quad (1)$$

where t_1 is the time spent by the liquid slug front moving from the upstream pressure transducer to the downstream one. L is the separation distance between two neighboring pressure taps. The slug length could be calculated by:

$$L_s = V_t t_2 - L \quad (2)$$

where t_2 is the difference between the time at which the liquid slug front contacts the upstream pressure tape and the time at which the liquid slug tail contacts the downstream pressure tape. It is assumed that the liquid slug length is constant in this time interval.

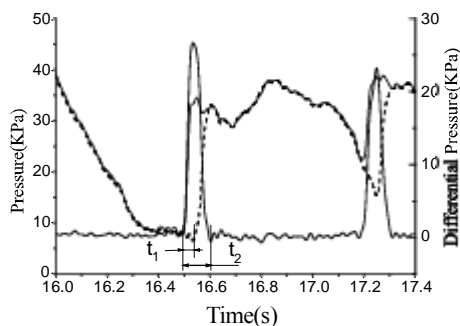


Fig. 3 Pressure and differential pressure vs. time

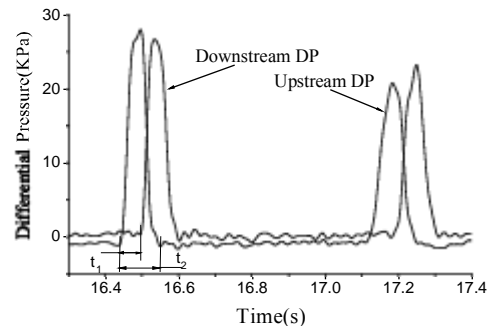


Fig. 4 Differential pressure vs. Time

3. FLOW PATTERN ONLINE IDENTIFICATION

3.1 Basic Principles of Flow Pattern Online Identification

The online recognition of flow regime need to measure real-time information of parameters, such as pressure, differential pressure, phase fraction and so on, at first, then to extract and analyze the feature of these, finally to make decision of what flow pattern it belongs to based on these feature. Choice of flow regime feature strongly affects the strategy of flow regime recognition and its accuracy. The flow

regime recognition method that is constituted of significantly different features will have a better performance as shown in Bai (1999), Huang & Zhong (1991). In fact we often don't know what feature is the most important, and we also can't make sure whether the pre-determined feature combination is appropriate. So feature extraction and analysis of signals is needed to find the most effective features to form a low-dimensional mode vector.

The basic principles of flow regime recognition are as followed:

(1) Sample sets which represent the flow regime feature should exist in the flow feature space of flow regime information,

$$\{X_{ij}\} \subset \{\varpi_k\} \quad (3)$$

where, $i=1,2,\dots,n$ is the kind of flow regime; $j=1,2,\dots,N$ is the flow regime samples composed of feature parameters; $k=1,2,\dots,M$ is the number of flow regime, $M=n$ is desirable. The principle includes the following meanings. The flow regime samples composed of feature parameters must be representative; Flow pattern samples should have the attribute property of a certain type of flow pattern, and it can express physical significance of the flow pattern to a certain extent; Feature parameters which react sensitively with flow regime can be chosen as pattern samples.

(2) The feature space should meet the principle of close cohesion for a certain flow regime mode, and far separation for different flow regimes mode. The less the distance in the same mode and the greater the distance among the different modes, the easier to separate different flow patterns will be.

According to this principle, feature extraction and analysis is conducted on the signals of pressure and pressure difference over a wide test range, which can be acquired easily in the industry. At the same time the clustering and separation characteristics of the feature parameter are studied. Then find the most effective feature to form the low-dimensional flow regime simple space and finally choose the concrete strategy to recognize the flow regimes on-line.

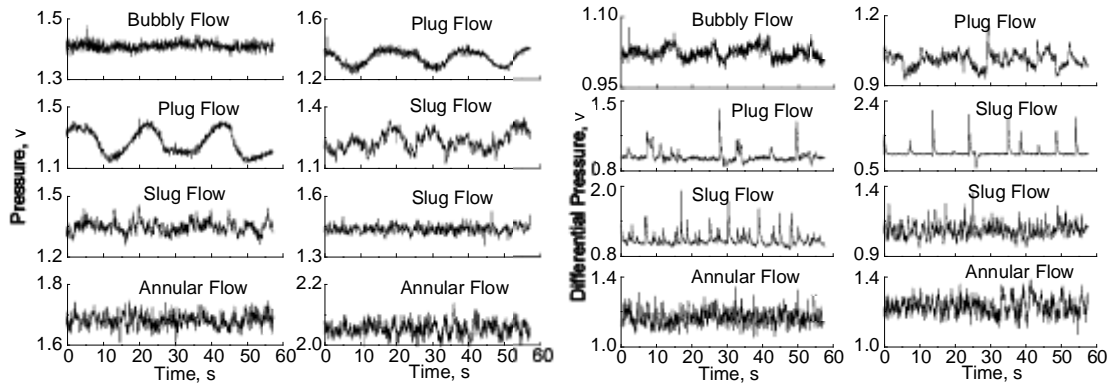
3.2. Feature Analysis and Flow Regime Recognition Rules

3.2.1 Feature Analysis

Experiment was conducted on oil-gas-water multiphase flow loop. The test section was made up of plexi glass pipe with the diameter of 40 mm and the length of 20 m. The measurement points of pressure and differential pressure located at 15 m section from the entrance. 40 # diesel was used during the experiment. The experimental range of oil fraction is from 0.11 to 0.75, the absolute pressure from 0.1 to 0.3Mpa, fluid temperature was 4 to 15°C, oil superficial velocity from 0.05 to 0.51 ms⁻¹, water superficial velocity from 0.05 to 1.51 ms⁻¹, and gas superficial velocity from 0.02 to 50.6 ms⁻¹. The experiment basically covered the range of industrial flow parameter under the medium velocity. Reference to the dividing method of two-phase flow of Mandhane, Gregory & Aziz (1974) and Acikgoz, Franca & Lahey (1992), and according to both visual observation and the fluctuating pressure and differential pressure, the oil-gas-water multiphase flow regimes in horizontal tube can be classified into four kinds: bubbly flow, intermittent flow, stratified flow and annular flow.

Since pressure and differential pressure signals contain a variety of noise, de-average value processing and filtering processing was done before feature extraction and analysis. Figure 5 shows a group of experimental results at oil superficial velocity of 0.05 m/s and water superficial velocity of 0.10 m/s. To bubble flow, the pressure and differential pressure fluctuations was small; To plug flow, the pressure signal was similar to rectangular wave and the differential pressure signal have a periodic rise; To slug flow, the rise frequency of differential pressure signal increase, whereas the periodicity of

pressure signal decrease; To annular flow, energy of pressure and differential pressure signal increase, the pressure and differential pressure signal don't have periods phenomenon no longer.



Run	Gas velocity	Flow regime	Run	Gas velocity	Flow regime
1	0.68	Bubbly	5	20.44	Slug
2	2.53	Plug	6	25.61	Slug
3	2.54	Plug	7	36.68	Annular
4	15.27	Slug	8	42.15	Annular

Fig. 5 Results at different pressure and differential pressure (see table as well)

Figures 6 and 7 respectively show the root mean square (RMS) features of the pressure signal and the variance features of differential pressure signal. Noting that the differential pressure signal is processed dimensionless, that is, divided by the differential pressure of the full tube water in order to remove the impact of diameter:

$$\Delta P = (\Delta P)_m / (\rho_w g D) \quad (4)$$

Where, ΔP , $(\Delta P)_m$, ρ_w , g , D are respectively the dimensionless differential pressure, average differential pressure (kPa), the density of water (kgm^{-3}), acceleration of gravity (ms^{-2}), and the diameter of the tube (m).

The change rule of pressure RMS is the same with that by Wambsganss, Jendrzeczyk, France (1991). Before the appearance of annular flow, RMS increases with gas velocity, but the liquid velocity has a non-monotonic influence. The RMS drops suddenly when the annular flow appears after the slug flow and increases with the liquid velocity. The RMS of differential pressure signal increases with the increment of gas velocity and liquid velocity. In addition, other feature parameters of pressure signal and differential pressure signal, such as the average deviation, the peak factor, the energy of every scale, fractal dimension, the biggest power spectrum, these all can't reflect the changes of flow regime. Increase the oil fraction, the relative velocity between gas and liquid will reduce, it can also restrain the bubble combination, the occurrence and development of interfacial wave, so it cause the above parameters even less sensitive to the change of flow regime.

3.2.2 The Recognition Rule of Flow Pattern

The flow regime surely exists in a certain feature space according to the basic rules of multiphase flow dynamics. The differential pressure fluctuation energy of annular flow and high speed intermittent

flow is higher than that of bubbly flow, stratified flow, etc. According to the dimensionless variance (total energy) of differential pressure signal, the flow regimes can be divided into two classes:

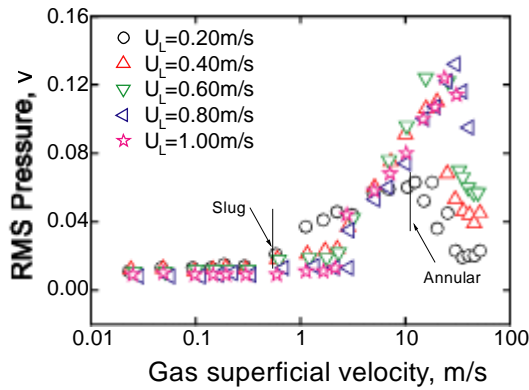


Fig. 6 RMS characteristin of the pressure signal(oil fraction is 0.2)

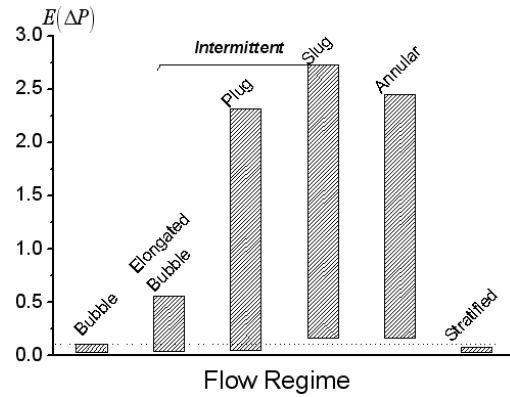


Fig. 7 Dimensionless variance of the differential pressure signal

$$E(\Delta P) \geq E(\Delta P)_c, \text{ for all annular flow and part of intermittent flow} \quad (5)$$

$$E(\Delta P) < E(\Delta P)_c, \text{ for all bubble flow, stratified flow and part of intermittent flow} \quad (6)$$

where, $E(\Delta P)_c = 0.12$.

Because the differential pressure can be measured directly, all feature parameters are unfolded on the dimensionless time-averaged differential pressure domain, and the law of these combined features is analyzed. Then the feature space of special flow pattern is established. Figure 8 indicates that the feature parameter of annular flow and part of intermittent flow (mainly slug flow and few plug flow) clusters together. As well, the feature parameter of bubble flow, stratified flow and part of intermittent flow (mainly plug flow and a few slug flows) gathers. The annular flow and intermittent flow is easy to be separated. The flow regime recognition rules can be established according to dividing these features space:

$$(\Delta P)_m \geq (\Delta P)_1, E(\Delta P)_c < E(\Delta P) \leq E(\Delta P)_1, \text{ annular flow} \quad (7)$$

$$(\Delta P)_m > (\Delta P)_2, E(\Delta P) \geq [E(\Delta P)_c, E(\Delta P)_2]_{\max}, \text{ intermittent flow} \quad (8)$$

In above equations,

$$E(\Delta P)_1 = 3.6 + 3.9\Delta P - 3.3(\Delta P)^2, E(\Delta P)_2 = -2.1 + 2.1\Delta P \quad (9)$$

$$(\Delta P)_1 = 3.2, (\Delta P)_2 = 2.8 \quad (10)$$

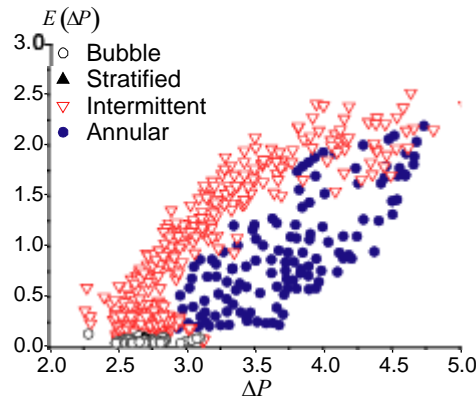


Fig. 8 Feature parameters unfolded on the differential pressure domain

3.3. Classification Machine of Flow Pattern

Although the flow regime recognition rule of the two regimes was put forward, the feature space of the two kinds still overlap. Therefore these flow regime rules are not suitable for all feature space. Moreover the feature spaces of other flow regimes overlap seriously. Other technique is needed to solve the problem. One of the solutions is to calculate the feature samples according to the experimental results with some algorithm, then compose feature space using these samples. The feature space can be used to identify the flow regime. Because the learning vector quantization (LVQ) classification machines have the character of self-organization, the present research chooses it to calculate the standard template of flow regimes. Suppose the euclidean distance between input sample x with the attribute ω_r and m_u which is the u -th sort is the nearest, then the iterative learning rule is as follows from Kohonen (1990):

$$m_i(k+1) = m_i(k) \quad (i = 1, 2, \dots, D) \quad \text{if } r = u \quad (11)$$

$$\begin{cases} m_r(k+1) = m_r(k) + \alpha(k)[x(k) - m_r(k)] \\ m_u(k+1) = m_u(k) - \alpha(k)[x(k) - m_u(k)] \end{cases} \quad \text{if } r \neq u \quad (12)$$

Where, $m(k)$ is template, D is the amount of template, $0 < \alpha(k) < 1$ is learning coefficient. The training samples $\{x_1, x_2, \dots, x_N\}$, the initial template vector $\{m_1(0), m_2(0), \dots, m_D(0)\}$ and the form of learning coefficient $\alpha(k)$ are all given. Of template samples $x_j \in \omega_r$, calculate the distance between x_j and all types of template samples and then find the minimum:

$$u = \arg \min_i \left\{ \|x_j - m_i(k)\|^2 \right\} \quad (13)$$

If $r=u$, the template vector of each kind is invariable, according to equation (9). Otherwise iterative calculate the quantitative vector of each kind of template, according to equation (10). Then standard template $m_i(k)$ of different flow pattern can be obtained if the iteration is convergent.

Fourier spectrum of pressure signal processed uniformly is selected to be the input vector of the learning vector quantization (LVQ) classification machines. When apply these standard templates to recognition unknown flow pattern, all distances between standard template and Fourier spectrum of the pressure signal of unknown flow regime should be calculated:

$$Z(x, m_i) = \|x - m_i\|^2 \quad i=1, \dots, D \quad (14)$$

Find the attribute of template quantization vector of the minimum distance, and the attribute is the sort of unknown flow regime.

3.4. Data Fusion Method of Flow Pattern On-line Recognition

3.4.1 Flow Process of Data Fusion

The pressure and differential pressure signal constitute the feature space of the flow regime recognition. The application of spectral analysis, statistical analysis and nonlinear analysis are limited in the space, it can only provide several kind of supposition set of flow regime recognition in certain knowledge scope. If the pressure and differential pressure signal features realize supplementary, the supposition set may reduce and approach to the real state and obtain the uniform description and the forecast of multiphase flow regime. Therefore, the success flow regime recognition method must be integration and fusion of the multi-sensor multi-characteristics and the knowledge. This research proposed one kind of solution according to multi-sensor data fusion technology as from Kohonen (1990) and Hall (2001). For pressure signal, the homogenized Fourier power spectrum, the root-mean-square and the fractal dimension number are extracted. For differential pressure signal, the time-domain characteristic such as dimensionless average value and the variance are extracted.

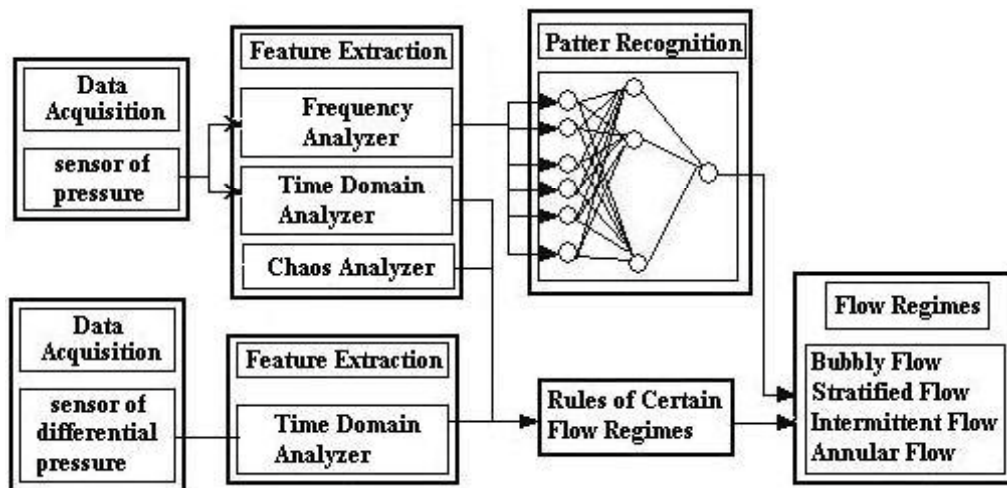


Fig. 9 Flow chat of the multi-sensot data fusion online recognition

Figure 9 shows the concrete flow chart of the multi-sensor data fusion online recognition of flow regime. First realize real-time measurement of pressure and differential pressure signal of multiphase flow, and then carry on the multi-feature extraction to the pressure and differential pressure signal, judge flow regime mode according to result of feature extraction and the recognition rules of specific flow pattern. If the flow regime feature does not satisfy the rule, take the learning vector quantization pattern classifier as the unknown flow regime classifier and complete the recognition according to standard template of the feature space.

The flow regime recognition method takes advantages of high confidence, good fault tolerance and less requirement of single sensor performance because of using the multi-sensor data fusion theory.

3.4.2 Flow Regime Online Recognition System and the Test Results and Analysis

According to the above flow regime online recognition theory, the flow regime recognition

instrument is developed using the micro-processing device, together with pressure, differential pressure sensors that layout on the pipeline, as well as the concurrent voltage source, these composed the flow regime online recognition system. The layout of measurement sensor is shown in Figure 10. This system does not change flow structure in pipelines.

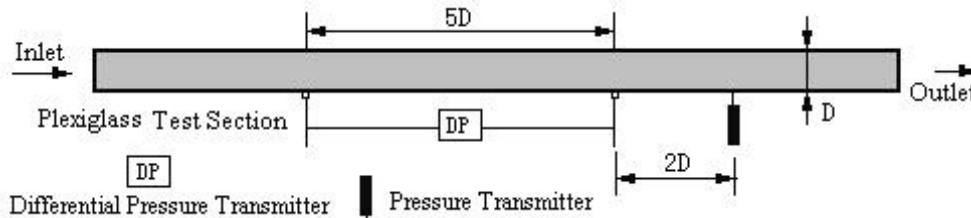


Fig. 10 Layout of measurement sensor in the flow pattern online recognition system

Carrying on the examination directly on the experiment system in laboratory, the test parameter area covered all scope of experiment flow parameter. To test the repeatability, we use three consecutive identify ways to the same condition. The test results are shown in Table1. In the wrong recognition, the annular flow was mistakenly identified as intermittent flow, the intermittent flow was mistakenly identified as annular flow, the bubbly flow and stratified flow, the stratified flow was mistakenly identified as intermittent flow and bubbly flow, the bubbly flow was mistakenly identified as intermittent flow and stratified flow. The total average flow regime correct recognition rate is 93.2%. In addition, the metrology institute measuring results show that the system has good duplication and good recognition accuracy rate, the recognition accuracy rate is as high as 96.7% except flow regime transition. With the experimental station of Daqing Oil Field Design Institute, using 80mm mixing pipeline and the crude oil-natural gas-water real fluid, the application results indicated that accuracy rate of flow regime online recognition was 91.3%.

Table. 1 Test result of oil-gas-water multiphase flow pattern recognition technology

Flow pattern	case number	Correct recognition	Correct rate
Annular flow	200	185	92.5%
Intermittent flow	400	377	96.8%
Stratified flow	50	46	90.2%
Bubbly flow	60	54	90.0%

The recognition method divided all flow regimes into four kinds, bubbly flow, stratified flow, intermittent flow and annular flow; it didn't define the flow regime transition as the new category. The test result indicated that accuracy rate of these 4 kinds of flow regime online recognition is higher than 90%. The wrongly distinguished flow regime mainly appeared at the transition region, the partial reasons are observer's subjective judgment, and the following research may consider the definition of flow regime transition. For the flow regimes under low air speed, such as bubbly flow, stratified flow, intermittent flow and so on, the pressure, differential pressure fluctuation energy is low, this cause high incorrect recognition rate, the following research might consider to layout differential-pressure sensor on the upper and lower sides of pipeline.

The flow regime recognition needs to obtain enough flow information. For the intermittent flow under low fluid velocity, its flowing periods may reach as high as above 10s. Therefore, the sampling time of the online recognition method of this research can't reduce at will.

4. AN EXPERIMENTAL AND NUMERICAL STUDY OF SLUG FLOW IN PIPE FLOW

Gas-liquid slug flow occurs frequently in the petroleum, chemical, civil and nuclear industries. It is characterized by a sequence of elongated bubbles separated by liquid slugs that may contain small bubbles. For its transient and intermittent nature, it is difficult to predict the flow characteristics correctly. Therefore, reliable flow models are crucial for the safe and cost efficient design and operation of industrial facilities.

In the offshore oil and gas field, the maximum slug length and its statistical distribution are very important for the design of separator and downstream processing facility at steady state operations. However transient conditions may be encountered in the production, such as operational upsets, start-up, shut-down, pigging and blowdown, which are key operational and safety issues related to oilfield development. So it is necessary to have an understanding the flow parameters under transient conditions. In this paper the evolution of slug length along a horizontal pipe in gas-liquid flow is studied firstly and then an experimental study of flowrate transients in slug flow is provided. Also, the special gas-liquid flow phenomena easily encountered in the life span of offshore oil fields, called severe slugging, was studied experimentally and some results are presented in this paper.

4.1 Slug Length Evolution of Gas-liquid Slug Flow in Horizontal Pipe

For steady state slug flow in horizontal pipe, Dukler & Hubbard (1975) presented the “unit cell” concept to predict average liquid fractions and pressure drops for given flow rates and pipe diameters. Several models based on this approach were developed later by other researchers to predict slug flow parameters. But all the models used constant slug length as the primary assumption and it is impossible to predict the slug length evolution along the pipe.

From visual observations, it is found that very short slugs generated at the entrance section of the pipe maybe have length of several diameters of the pipe. However the frequency of the slugs is relatively high. When the short slugs move downstream along the pipe, some elongated bubbles disappear and short slugs merge to form longer slugs. In this process frequency of slug reduces and reaches a stable one when most slugs are long enough and can flow out of the pipe. The surviving of slug is controlled by the pick-up process at the slug front, where the moving slug front scoops the liquid film under the large gas bubble, and by the liquid shedding process at the tail of the slug. The liquid shedding rate is determined by the translational velocity of the Taylor bubble of the slug unit, while the translational velocity is related to the maximum local velocity of the slug tail. At the tail of short slug, the velocity profile is not developed fully as the long one, therefore short slugs are unstable and are easily overtaken by the following Taylor bubble (Moissis & Griffith 1962). When a short slug disappeared, the liquid is scooped by the approaching slug and its length increases. Moissis & Griffith (1962) studied the rate of collapse of liquid slugs due to wake effect in upward vertical flow. Cook & Behnia (2000) studied this effect in near horizontal pipe. It is interesting that both their results can be regressed in the form of exponential expression.

From field data Brill et al. (1981) found the slug length followed a log-normal distribution and Nydal et al. (1992) also had the same conclusion from experimental data. Zheng et al. (1994) proposed a simple slug tracking model to simulate slug flow in hilly terrain pipeline. The model applied source and sink concepts to the elbows between pipe sections which have different inclinations. Barnea & Taitel (1993) also used a simple slug tracking model to calculate slug evolution along vertical pipe. In their model an assumption relation of the translational velocity between neighboring liquid slugs is used to consider the wake effect. Cook & Behnia (2000) compared the experimental slug length distribution in near horizontal pipe with this model and found the agreement was very well. Hout et al. (2001) studied slug length distributions in upward vertical flow. In the model presented by Barnea & Taitel, the film surrounding the Taylor bubble zone and the small gas bubbles in liquid slug are neglected.

In 1996, Nydal and Banerjee developed a Lagrangian slug tracking model, which is based on the integral balances of mass and momentum of the liquid slug and gas bubble in a slug unit. An important assumption is that there is no gas was entrained in the liquid slug. The program of this model is implemented with object oriented technique. The predicted results of hilly terrain slug flow from this model agreed well with measured data. Taitel and Barnea (1998, 1999) proposed a slug tracking model which based on the unit cell model presented by Dukler and Hubbard. This is a Lagrangian model and could record trajectories of every slug and Taylor bubble in the pipe. In this model, liquid film was assumed to have an averaged equilibrium height to simplify the calculation and the acceleration pressure drop, which is brought by the velocity increase of the liquid film scooped by the next liquid slug, is not considered.

In the present work, the Taitel and Barnea model is modified to considered the acceleration pressure drop and programmed in C++ with object oriented technique. The evolution of slug length along pipe of hydrodynamic slug flow was studied experimentally in a horizontal pipe and numerically by the simulator.

4.2 Slug Tracking Model

The model proposed by Taitel & Barnea(1998,1999) was adopted and modified to consider the acceleration pressure drop in this paper.

The slug tracking model was based on the mechanistic “unit cell” concept presented by Dukler and Hubbard(1975). A typical slug unit consists of a liquid slug zone of length L_s and an elongated bubble zone of length L_f . There is a liquid film under the long gas bubble. The main assumption of the “unit cell” model is that slug flow is comprised of a series of slug units in which every liquid slug has the equal length. However in the tracking model each liquid slug has its individual length and the velocities of liquid slug front and tail are calculated respectively. Therefore the lengths of all slugs in the pipeline can be determined. In the pipe some slugs might disappear when their lengths are shorter than a critical length and two neighboring elongated bubbles would be merged. To simplify the calculation a uniform equilibrium film height is used.

As shown in Fig. 11 the position of liquid slug front is Z_{fr} and the tail is Z_{ta} . The velocities of liquid slug front and tail are U_{fr} and U_{ta} respectively. These parameters as well as the fluid velocity, pressure and holdup in every liquid slug and liquid film and the gas velocity in elongated bubble are calculated. In the tracking model, the slug unit at the entrance is calculated by the steady state “unit cell” model and its slug length is specified, while in the pipe the lengths of liquid slug and liquid film are calculated by the velocities of liquid slug front and tail from the former time step. In this paper, some modifications of the Taitel and Barnea model are presented.

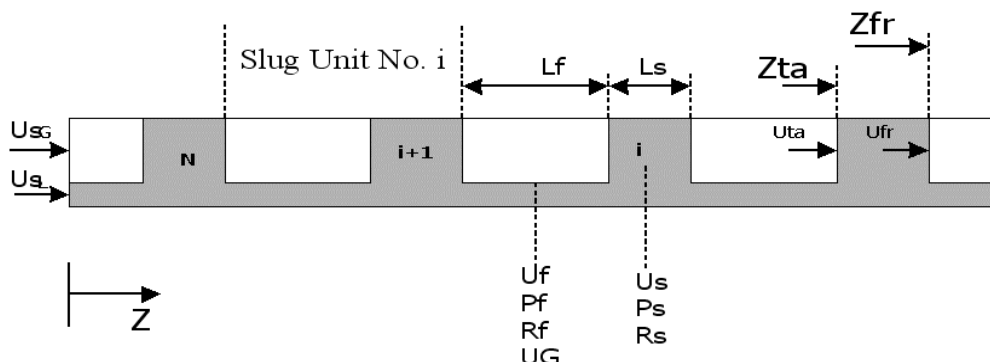


Fig. 11 Simplified diagram of slug flow structure in horizontal pipe

4.2.1 The Translational Velocity and the Wake Effect

The translational velocity of an elongated bubble following a developed liquid slug has been studied extensively. The well known relation proposed by Nicklin et al. (1962) has been applied for all pipe

inclinations. In this study the translational velocity was also analyzed and it was found that the following correlation can be used:

$$V_t = 1.2V_m + 0.54\sqrt{gD} \quad (15)$$

Due to the wake effect, the translational velocity of elongated bubble will increase as the liquid slug length in front of it decreases. Cook & Behnia (2000) experimentally studied it near horizontal pipe and obtained a correlation. The highest mixture velocity used in their experiments was 2.5m/s. In this work their correlation is applied to consider the wake effect:

$$\frac{V_{tb}}{V_{t\infty}} = 1.0 + 0.56 \exp\left(-0.46 \frac{L_s}{D}\right) \quad (16)$$

where $V_{t\infty}$ is the translational velocity of long bubble following a liquid slug of stable length, calculated from Eq.(???) L_s is the length of the liquid slug separated the neighboring elongated bubbles.

4.2.2 Pressure Drop Calculation

In this work the acceleration pressure drop due to slug front scooping film liquid ahead of it is considered. The pressure drop is calculated by force balance. Bendiksen (1996) described that the mixing zone at the slug front is short when the mixture velocity is low, but when the mixture velocity is high the mixing zone is long and maybe has half the slug length. To simplify the problem, we assume that the acceleration pressure drop distributes over half of the liquid slug. By the force balance between the pressures of the point i and $i+1$, it gives:

$$\begin{aligned} P_{S_{i+1}} = & P_{S_i} + \frac{1}{4} f_{S_i} \rho_{S_i} L_{S_i} \frac{S}{A} |U_{S_i}| U_{S_i} + \frac{1}{2} \rho_{S_i} g \sin \phi L_{S_i} \\ & + \frac{1}{4} f_{S_{i+1}} \rho_{S_{i+1}} L_{S_{i+1}} \frac{S}{A} |U_{S_{i+1}}| U_{S_{i+1}} + \frac{1}{2} \rho_{S_{i+1}} g \sin \phi L_{S_{i+1}} \quad (17) \\ & + \left[\frac{\tau_f S_f}{A} + \frac{\tau_G S_G}{A} + \rho_f g \sin \phi \right]_{f_i} L_{f_i} + \Delta P_{acc_{i+1}} \end{aligned}$$

where the acceleration pressure drop is (Sharma, Y. 1985) given by:

$$\Delta P_{acc} = \rho_L R_s (U_s - U_f)(V_t - U_s) \quad (18)$$

At each time step, the variables $P_{S_{i+1}}$, P_{S_i} , U_{S_i} , $U_{S_{i+1}}$ are unknown and the other variables are taken from the previous step. The equation used to linearize last two equations is:

$$|U_{S_i}^{new}| U_{S_i}^{new} = 2|U_{S_i}| U_{S_i}^{new} - |U_{S_i}| U_{S_i} \quad (19)$$

Therefore Eq. (18) can be written:

$$\begin{aligned} \Delta P_{acc\,i+1} &= \rho_{L\,i+1} R_{S\,i+1} (U_{S\,i+1} - U_{f\,i}) (U_{t\,a\,i+1} - U_{S\,i+1}) \\ &= \rho_{L\,i+1} R_{S\,i+1} \left[\begin{aligned} &(U_{f\,i} + U_{t\,a\,i+1}) U_{S\,i+1} - U_{f\,i} U_{t\,a\,i+1} \\ &- 2U_{S\,i+1} U_{S\,i+1}^{new} + U_{S\,i+1}^2 \end{aligned} \right] \end{aligned} \quad (20)$$

Thus the discretization form of Eq. (17) is:

$$\begin{aligned} P_{S\,i}^{new} &+ \left[\frac{1}{2} f_{S\,i} \rho_{S\,i} L_{S\,i} \frac{S}{A} |U_{S\,i}| \right] U_{S\,i}^{new} + \left[\begin{aligned} &\frac{1}{2} f_{S\,i+1} \rho_{S\,i+1} L_{S\,i+1} \frac{S}{A} |U_{S\,i+1}| \\ &- 2\rho_{L\,i+1} R_{S\,i+1} U_{S\,i+1} \end{aligned} \right] U_{S\,i+1}^{new} \\ - P_{S\,i+1}^{new} &= -\frac{1}{2} \rho_{S\,i} g \sin \varphi L_{S\,i} - \frac{1}{2} \rho_{S\,i+1} g \sin \varphi L_{S\,i+1} \\ &+ \frac{1}{4} f_{S\,i} \rho_{S\,i} L_{S\,i} \frac{S}{A} |U_{S\,i}| U_{S\,i} + \frac{1}{4} f_{S\,i+1} \rho_{S\,i+1} L_{S\,i+1} \frac{S}{A} |U_{S\,i+1}| U_{S\,i+1} \\ &- \left[\frac{\tau_f S_f}{A} + \frac{\tau_G S_G}{A} + \rho_f g \sin \varphi \right]_{f\,i} L_{f\,i} \\ &- \rho_{L\,i+1} R_{S\,i+1} \left[(U_{f\,i} + U_{t\,a\,i+1}) U_{S\,i+1} - U_{f\,i} U_{t\,a\,i+1} + U_{S\,i+1}^2 \right] \end{aligned} \quad (21)$$

where ρ_f is defined by:

$$\rho_f = R_f \rho_L + (1 - R_f) \rho_G \quad (22)$$

The slug tracking model was abstractly analyzed with object oriented technique and programmed in C++ language. All the liquid slug and elongated bubble in the pipe are managed by a double linked list.

4.2.3 Results and Discussion

Liquid slug lengths were measured by the differential pressure method from the experiments covering a wide range of mixture velocities. The pressure signals to determine the slug lengths were measured from P11, P12 and P13. Fig. 10 shows the maximum, minimum and mean slug length versus to the local superficial mixture velocity. From the experimental data the liquid slug lengths were collected and the statistical result was obtained:

The mean slug length ranges from 8.3~19D; the averaged value is 13D.

The maximum slug length ranges from 22~36D; the averaged value is 31D.

The minimum slug length ranges from 2~11D; the averaged value is 4.3D.

The error bars show in Fig. 12 represents the standard deviation of the mean slug length. From Fig. 12 it is clearly shown that the slug length is not dependent on the mixture velocity, which agrees well with the work of many former researchers.

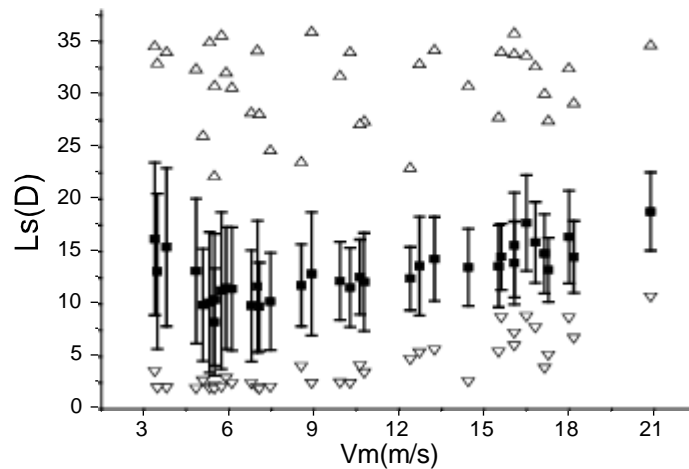


Fig. 12 Measured maximum(Δ), minimum(∇) and mean(\blacksquare) slug length. The error bars represent the standard deviation of the mean slug length

In order to get accurate statistical distribution of liquid slug length, some experiments run for a very long time and several hundreds of liquid slugs were recorded. Fig. 13 presents the observed liquid slug length distributions which were measured at 12.83m, 16.83m and 18.83m from the pipe entrance respectively. The air and water superficial velocities are 7.3m/s and 1.52m/s respectively. The liquid slug length distributions calculated by the simulator are also shown in Fig. 14 and represented by shadow filled columns. The model used a normal distribution of liquid slug length between 2D and 3D entering the pipe. Comparison with the measurements in Fig. 13, it is clear that the predicted slug length distributions are very good and both Fig. 13 and Fig. 14 show a right-skewed distribution for slug length. The maximum and the averaged slug length and its standard deviation are given in both figures for each measured results. The numbers of slugs involved in the calculation process are also shown in Fig. 14.

As shown in Fig. 13, both the averaged and the maximum slug length increase along the pipe. In Fig. 14, the number of simulated liquid slugs reduced 53 from 12.83m to 16.83m after the pipe entrance, i.e. averaged 13.3 per meter, while from 16.83m to 18.83m the slugs reduced 20, i.e. averaged 10 per meter. It was distinctly shown that short slugs disappeared during the liquid slugs flowing along the pipe and the slug lengths tended to stabilized at a longer length. When some short slugs disappeared, the other slugs would scoop the liquid shed by the decaying slug and their lengths increase, therefore both the mean and the maximum slug length increased along the pipe. The calculation agrees well with the measurements. The agreement between the predicted maximum slug length and the measured is also quite good.

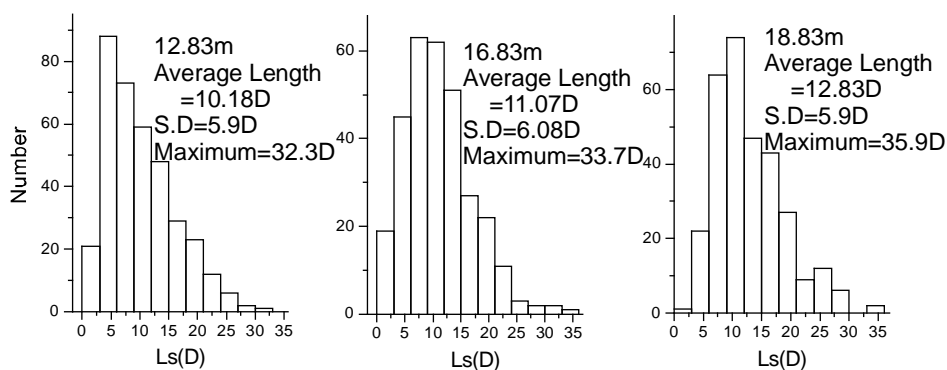


Fig. 13 Measured slug length distributions at 3 positions along the pipe
 ($V_{SL}=1.52\text{m/s}$, $V_{Sg}=7.3\text{m/s}$)

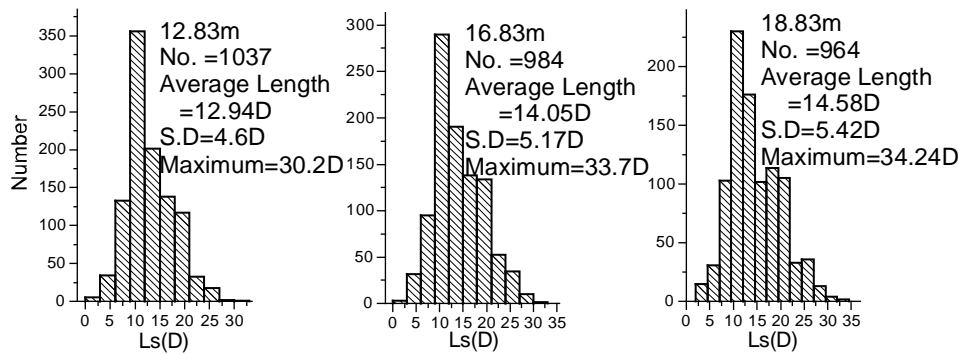


Fig. 14 Predicted slug length distributions at 3 positions along the pipe
 ($V_{SL}=1.52\text{m/s}$, $V_{Sg}=7.3\text{m/s}$)

But the predicted averaged slug length is higher than the measured length and the mean difference is 2.5D. This difference may be due to the separation effect of the U-type elbow (Fig. 2). When a slug is passing in the elbow pipe, in addition to the gravitational force there is centrifugal force put on the liquid slug. For the stronger volume force on the slug in the elbow liquid, liquid in the slug will be distributed to the film zone thereby the slug length will decrease. For short slugs this effect would be more effective because both the front and tail of liquid slug locate in the elbow pipe. Whereas for long slugs, such as the maximum slug, their lengths are longer than the elbow pipe length (about 25D) and it means that at least one of the ends of slug is not in the elbow pipe section and this will prevent these liquid slugs in the elbow section from decreasing in length. Hence the separation effect of the elbow on the maximum slug is very little. On the other hand, the start of slug flow from stratified flow need a small distance from the entrance, but it is not considered in the simulator and this also might increase the predicted mean slug lengths. From 12.83m to 16.83m after the entrance, the increase of the measured mean slug length is 2.65D, while the predicted is 1.64D, so it is clear that the elbow blocks development of the slug flow.

Fig. 15 and 12 are the measured and the predicted slug length distribution when the air and water velocities are 8.93m/s and 0.98m/s respectively. The predicted mean slug length is 2.57D longer than the measured, which is similarly with the former case. The difference of the maximum slug lengths between the observed and the predicted is only 1.34D. Fig. 15 and 12 also present the shape fitted to the measured distributions of the liquid slug lengths. It was found that both measured and predicted distributions follow a log-normal distribution. The both fit equations are given:

Measured liquid slug lengths:

$$\bar{y}\left(\frac{L_s}{D}\right) = 0.00577 + 0.255 \exp\left(-\frac{\ln^2\left(\frac{L_s}{11.472D}\right)}{2 \times 0.238^2}\right) \quad (23)$$

Predicted liquid slug lengths:

$$\bar{y}\left(\frac{L_s}{D}\right) = 0.0154 + 0.28498 \exp\left(-\frac{\ln^2\left(\frac{L_s}{12.945D}\right)}{2 \times 0.15334^2}\right) \quad (24)$$

To understand the disappearing and merging process of the liquid slugs and the elongated bubbles close to the entrance, the moving trajectories of 8 slugs and 8 bubbles were recorded in about 0.35s

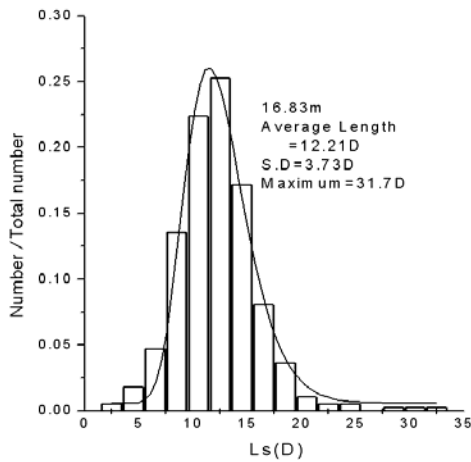


Fig. 15 Measured slug length distribution,
 (—)log normal fit
 ($V_{SL}=0.98\text{m/s}$, $V_{Sg}=8.93\text{m/s}$)

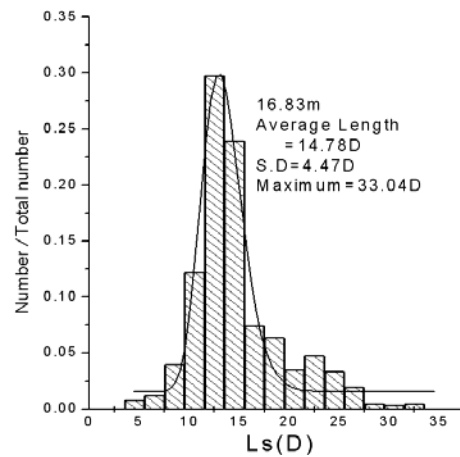


Fig. 16 Predicted slug length distribution,
 (—)log normal fit
 ($V_{SL}=0.98\text{m/s}$, $V_{Sg}=8.93\text{m/s}$)

from one calculated case as shown in Fig. 12. Fig. 17 shows the trajectories of all slugs and elongated bubbles vs. time in 0.35s. There were 8 slugs entering the pipe, but only the third and the eighth liquid slug flowed out of the pipe successfully. Four liquid slugs preceding the eighth liquid slug disappeared and the shed liquid is collected by the eighth liquid slug in the process, thus its length increased and the stable length was reached after the velocity of front was equal to the tail velocity. At the same time, five bubbles merged and formed a long one before the eighth liquid slug. The third liquid slug collected the liquid from the first and the second liquid slug, therefore its length was shorter than the eighth liquid slug.

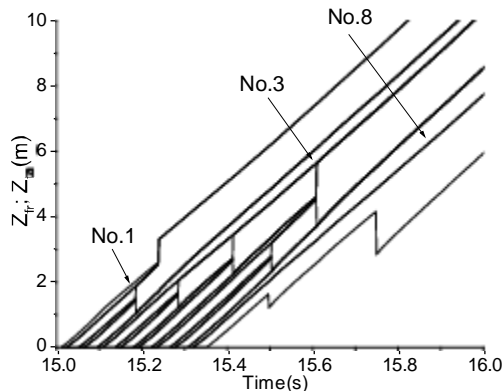


Fig. 17 Predicted slugs and elongated bubbles trajectories($V_{SL}=1.52\text{m/s}$, $V_{Sg}=7.3\text{m/s}$)

4.3 An Experimental Study of the Flowrate Transients in Slug Flow

Slug flow is of crucial significance as a great number of multiphase transport lines are operated in this flow regime. The flowrate transient with slug flow is widely met in oil and gas pipelines. For steady state operations, parameters such as holdup and pressure gradient are important, whereas under transient conditions, an understanding of additional parameters such as maximum slug length and peak pressure is also required.

Transient conditions include operational upsets, start-up, shut-down, pigging and blowdown, which are key operational and safety issues related to oilfield development. Flowrate transient phenomena

mean that the mass flux of two-phase at inlet or outlet changes with time. They may be classified into slow transient and fast transient condition depending on whether the state of fluids is in steady state. Under slow transient, the state of fluid at every location of the pipeline is in steady or quasi-steady state so that the fluid flow can be modeled by a steady state or quasi-steady state approach. Under fast transient, the fluid flow and its state parameters in every location of pipeline can not be modeled by a steady state or quasi-steady state approach and have to be dealt with by a special method. In a pipeline for oil and gas transportation, the flowrate change caused by the fluctuations of pressure beneath the well and the liquid height of downstream separator or storage tank is called slow transient, whereas the flowrate change caused by man-controlled fast operations and other accidents is called fast transient. Usually, the flowrate transient is accommodated with the changes of liquid and gas fluxes simultaneously, but, for convenience of research, the experiment was designed and operated in such a way that the change of mass flux was in one phase first, then in two phases simultaneously. We examined the effect of a step change in one of fluid flowrates of two phases. Five types of transients, i.e., “Up-gas” transient, “Down-gas” transient, “Up-liquid” transient, “Down-liquid” transient and simultaneously change of gas and liquid mass flux, were simulated in our experiments.

The effects of flowrate transients in horizontal pipes have been studied for a number of years. Sakaguchi et al (1973) looked, in particular, at the formation of slugs in flowrate transients between two steady states of stratified flow. Taitel et al (1978) conducted a more detailed study of air and water flowrate transients in a pipe with 38.1 mm internal diameter. Caussade et al (1987) conducted an air-water two-phase flow experiments in an 89.9 m long pipeline of 53 mm internal diameter, in which the void fractions and pressures were recorded at five locations along the test section. Their experimental results showed the propagation of both pressure and holdup waves along the pipe. For the gas flow transients, a pressure overshoot beyond the value of the new steady state was observed at the entrance to the test section, but not apparent at the exit. Minami (1991) conducted a flowrate transients experiment in slug flow regime using air and kerosene in a 3-inch diameter pipeline of 420 m length. He pointed out that an around 30 kPa pressure overshoot was identified in the entrance of test section for a gas flowrate increase transient and associated with an increased liquid discharge rate corresponding to a period of intense slugging, and about 500 s was needed to establish a new steady state. In the case of gas flowrate decreasing transient, the pressure undershoot below the new steady state was around 25 kPa and the liquid build-up in the separator appeared to be consistent with the existence of a period of stratified flow.

More recently, King et al (1996) presented preliminary findings for flowrate transients within the slug flow regime in WASP(Water, Air, Sand, Petroleum) facility of Imperial College. They concluded that gas transients exhibit pressure and holdup effects and that decreasing gas transients caused the temporary formation of a stratified flow. Liquid transients caused changes in slug frequency with smooth pressure changes between the steady states. King et al (1998) considered the large-scale or ensemble-averaged response of a slug flow to inlet flowrate changes in the same facility and observed the response of individual slugs to flowrate changes using a series of conductivity probes along the test section. This allowed a detailed study of the growth and collapse of individual slugs under transient conditions to be undertaken.

All of above-mentioned researchers observed the change of characteristic parameters in the flowrate transients, but did not give out any quantitative relationship between the changes of characteristic parameters and flowrate.

In this work, we investigate the large-scale or ensemble-averaged response of a slug flow and the response of individual slug to inlet flowrate changes using a series of pressure transducers and differential pressure transducers along the test section. The quantitative relationships between the changes of characteristic parameters and flowrates are obtained from the experimental results.

4.3.1 Test Loop and Experimental Method

A schematic diagram of the facility located at the University of Petroleum(East China) is shown in Fig.18. The rig can be operated at pressure up to 1200 kPa using air-oil-water three-phase flow as

working fluid, in which air was powered by a frequency modulation compressor, water was supplied by a centrifugal pump from water tank, and the oil was driven by a screw pump. The compressor was controlled by the mode of frequency modulation according to the fluctuation of gas pressure in buffer tank to maintain the pressure constant. The regulating valves were used to maintain the flow velocity constant. A vessel slug catcher and a multiple-pipe slug catcher were installed in the end of test section and all were controlled by regulating valves and computer. The present experiment was limited to air-water flow under 100 kPa to 200 kPa at the exit of system. The test section is a stainless steel pipe with 378 m length and 80mm inner diameter.

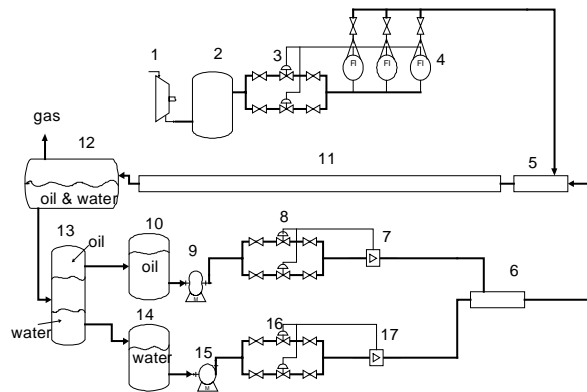


Fig. 18 A schematic of the experimental system

- 1—frequency modulation compressor; 2—gas buffer tank; 3—gas regulator; 4—metal rotameter;
- 5—gas & liquid mixer; 6—oil-water mixer; 7—ROSEMOUNT mass flowmeter; 8—oil regulator;
- 9—screw pump; 10—oil tank; 11—experimental section; 12—gas-liquid separator;
- 13—oil-water separator; 14—water tank; 15—centrifugal pump; 16—water regulator;
- 17—ROSEMOUNT mass flowmeter

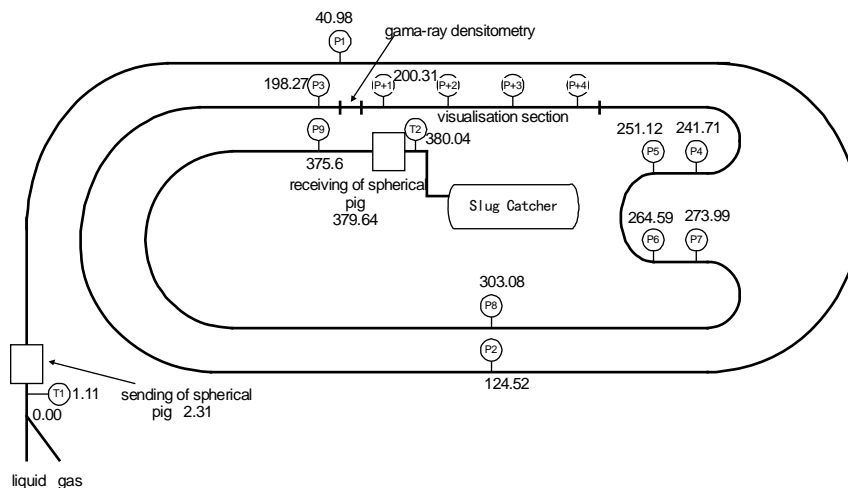


Fig. 19 Location of measuring instruments

Two ROSEMOUNT mass flowmeters (model CFM100 M328NU and CFM100 M328NU, accuracy $\pm 0.1\%$) and three Metal Rotameters (model H54, accuracy class 1) were used for the flowrates measurement of every fluid phase before entering the mixers. Then the fluids were respectively introduced into mixers to form two or three phase flow. A serial of KELLER PA23e pressure transducers and a gama-ray densitometer were installed in the test section for identification of

flow pattern and measurement of pressure and liquid holdup as shown in Fig.19. Ten KELLER PA25e pressure transducers $P_0 \sim P_9$ were arranged respectively at nine locations along the test section, P_0 was located at the inlet of the gas flowmeter to measure the gas pressure and four KELLER PA25e pressure transducers $P_{+1} \sim P_{+4}$ were used for the measurement of slug velocity and slug length. The changes of pressure associated with flowrate transient were measured using above mentioned pressure transducers of KELLER PA25e model. Their frequency response is 5000 Hz, which is high enough to pick up the characteristics of pressure change. The signal from the flowmeters and pressure transducers were sampled by a model PCI-6071 data acquisition system from NATIONAL INSTRUMENTS. The sampling frequency of each channel is 2500Hz.

As described by King et al. (1998), the upstream compressible volume has an effect on the flowrate transients. To minimize this effect the gas and liquid flows were throttled through the regulator valve before flowing through the part for flowrate measurement of test loop.

4.3.2 Gas Flowrate Transients

We study the effect of a step increase or decrease in the flowrate of gas (called “up-gas” transients or “down-gas” transients) on the flow regime and characteristic parameters of slug flow first. Although the flow regime transition can occur during the transient process the new steady state is also in the slug flow regime after a flowrate increases or decreases. During the gas flowrate transients, the pressure of gas buffer tank in the loop is maintained at 800 kPa and the liquid regulator is at rest. According to change of gas flowrate, the gas regulator was adjusted and controlled by a computer program to make the flow reach a new steady state.

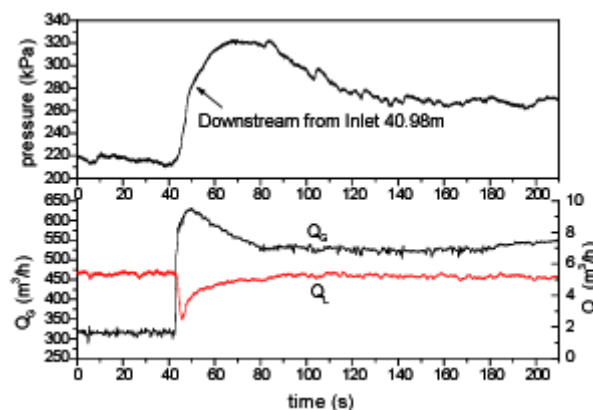


Fig. 20 Flowrate and pressure in “Up-gas” transient

4.3.2.1 Analysis of Pressure Fluctuation

(1) “UP-GAS” transients

Fig.20 shows a typical result of pressure profile with time at the location of 40.98 m away from the entrance in “up-gas” transient. A peak of gas flowrate was found between the initial steady state flowrate $315.3 \text{ Nm}^3 \cdot \text{h}^{-1}$ and final steady state flowrate $523.1 \text{ Nm}^3 \cdot \text{h}^{-1}$. The peak of gas flowrate was $632.2 \text{ Nm}^3 \cdot \text{h}^{-1}$. At the moment of 40.6 s, the gas flow rate increased rapidly to reach the peak, then decreased slowly and continued for 36.8 s to reach the final steady state. As the gas flowrate increased, the liquid flowrate decreased from $5.35 \text{ m}^3 \cdot \text{h}^{-1}$ to $2.46 \text{ m}^3 \cdot \text{h}^{-1}$ rapidly, though the liquid regulator did not take any action. This is not desirable but inherent characteristics in our system.

At the beginning of the “up-gas” flowrate transient, the pressure in pipeline increased rapidly almost at the same time. As soon as the peak value reached, the pressure decreased slowly from the peak value and continued for 136.3 s before reaching the new steady state. This phenomenon is called pressure overshoot. Under the conditions of $315.3 \text{ m}^3 \cdot \text{h}^{-1}$ for gas flowrate and $5.35 \text{ m}^3 \cdot \text{h}^{-1}$ for liquid flowrate, the value of pressure overshoot is 56 kPa at the location 40.98 m away from entrance.

The reason for this feature is that there exist different response speeds of the pressure build-up and the acceleration of liquid slugs. According to the idea of Nicklin et al. (1992), the slug velocity is always represented as a sum of two terms as follows:

$$V = C_0 V_m + V_\infty \quad (25)$$

where V_∞ is the drift velocity and V_m is the homogeneous mixture velocity. Therefore, the slug velocity is directly proportional to the homogeneous mixture velocity which equals to the sum of liquid superficial velocity V_{SL} and gas superficial velocity V_{SG} . The increase of gas flowrate results in an increase of slug velocity. However, inertia of liquid slugs has a baffle to its acceleration. This must induce a larger acceleration pressure drop and cause a pressure overshoot above the new steady state. This additional pressure drop is directly proportional to the change of the homogeneous mixture velocity.

The value of pressure overshoot is a function of the gas flowrate change, gas slug volume and others. The more the gas flowrate change is and the less the downstream gas slug volume is, the more the value of pressure overshoot is.

Table. 2 The pressure overshoot at different location from entrance

Distance, m	Pressure overshoot, kPa
-22	53
40.98	56
124.5	67.8
198.3	76.3
241.7	83.7
251.1	83.1
264.6	85.1
274	86.9
303.1	80.4
375.6	66.4

Table 2 presents the relationship of the value of pressure overshoot and the distance from the entrance. The value of the pressure overshoot increases with the distance but decreases at the location close to the exit. The reason is that with the decrease of pressure along the pipeline, the gas volume in slug and the slug velocity increase, so that the pressure drop for mixture acceleration increases to overcome the inertia of liquid slugs. Because there may be no liquid slug or only one liquid slug at the location near the exit of pipeline, the value of pressure overshoot is lower than that at upstream locations. At the upstream location of the pipeline exit, the interaction between two nearby liquid slugs is not negligible.

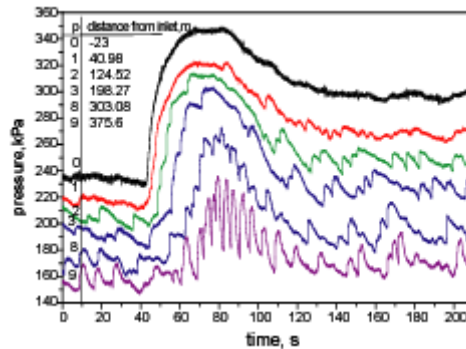


Fig. 21 Pressure profile of different locations

The pressure in test section is a function of the number of slugs, length of slug, slug velocity and the distance between measuring location and the exit of pipeline. The increase of gas flowrate results in a pressure increase. However there exists a time delay for the pressure increase between two different locations due to the damp of gas slug. Fig.21 shows the pressure profiles at different locations in pipeline. The “up-gas” flowrate transient is often associated with the formation of a larger slug. This is consistent with that the increased gas flowrate promotes the formation of a slug which sweeps down the pipeline with a higher gas driving velocity behind the slug, which forcing it over a relatively high holdup in front of the slug. A new steady state slug is being effectively pushed over a higher film holdup than the old steady state one. Under these circumstances, the possibilities for extremely rapid slug growth are increased.

Table 3 presents the spread speed of pressure wave obtained using an approximate method. The spread speed of pressure wave decreases along the pipeline.

Table. 3 Spread speed of pressure wave at different locations

Distance from entrance, m	Pressure wave speed, m.s ⁻¹
82.74	16.22
161.4	10.87
220	9.528
257.9	9.32
288.6	9.25
339.4	7.85

(2) “DOWN-GAS” transients

Figure 22 shows a typical pressure profile at the location 40.98 m away from the entrance under “down-gas” transients. The phenomena occurred during “down-gas” transient are different from those during “Up-gas” transient. With decreasing gas flowrate, the pressure at different location of the pipe reduced almost simultaneously and reached a valley below the value of final steady state. This phenomenon is called pressure undershoot. The main reason is that as the gas flowrate decreases, the velocity of liquid slug reduces to one below that of downstream slugs, then the volume of gas slug between two nearby liquid slugs increases, gas expands and the pressure reduces to one less than that in the new steady state.

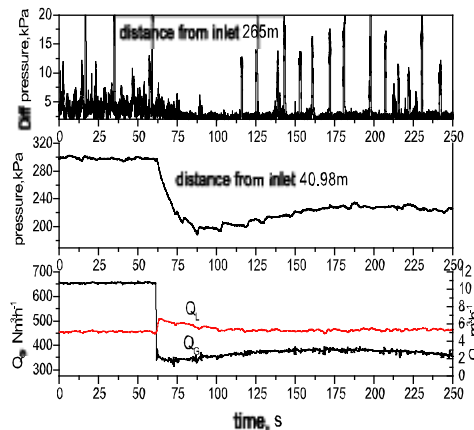


Fig. 22 Flowrate and pressure in “Down-gas” transient

The value of pressure undershoot is sensitive to the flow condition and magnitude of gas flowrate change. Except that, the value of pressure undershoot is related to the locations of pipeline Figure 23 and Table 4 show the change of pressure undershoot with the distance away from the entrance. As the distance away from pipeline entrance increased, the values of pressure undershoot increased at first, then decreased linearly.

During the “down-gas” transient, the slug velocity decreased rapidly. Since these slugs were already existed in the test section when the transient initiated, the liquid layer in front of these slugs retained the low thickness feature corresponding to the previous higher gas velocity. These slugs picked up less liquid from the thin layer than when they shed from their tails, so that they collapsed rapidly and led to a short period of stratification. As shown in Figure 23 and Table 4, the period of stratified flow is a function of the distance away from the entrance. The further the distance is, the longer the period of stratified flow is.

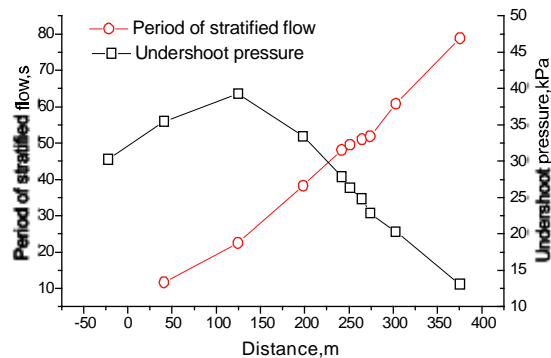


Fig. 23 The value of pressure undershoot and the period of stratified flow versus distance

Table. 4 The value of pressure undershoot and the period of stratified flow at different locations of pipeline

Distance from entrance,m	Pressure undershoot, kPa	Stratified Period,s
-22	30.2	11.71
40.98	35.5	22.54
124.5	39.28	38.25
198.3	33.41	48.126
241.7	27.86	49.53
251.1	26.33	51.05
264.6	24.81	51.87
274	22.86	60.79
303.1	20.29	78.84
375.6	13.08	11.71

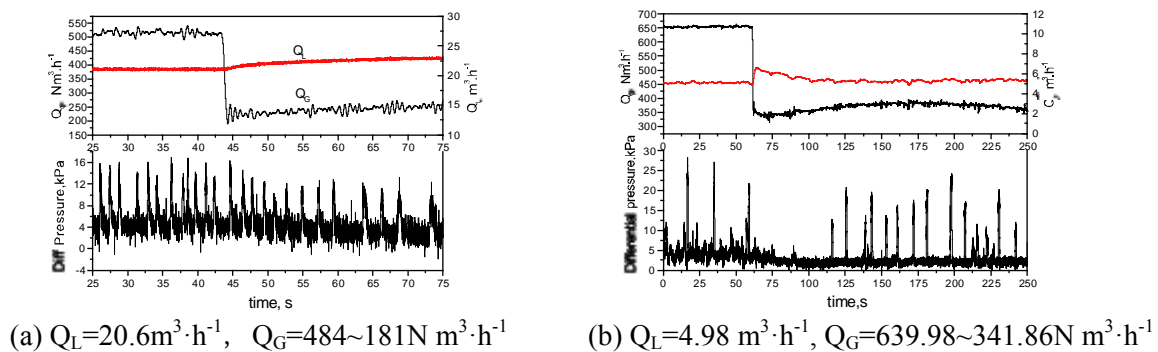


Fig. 24 Differential pressure fluctuation at same point

Except the distance away from the entrance, the liquid superficial velocity has an important influence on the period of stratified flow. The greater the liquid superficial velocity is, the shorter the period of stratified flow appears to be. This is an extension of the natural slug frequency cycle; a higher superficial liquid velocity corresponds to a higher slug frequency and thus the liquid layer recovers more quickly to the new equilibrium value corresponding to the inlet holdup (1977). Fig.24 shows the differential pressure profiles at different liquid superficial velocities. In Fig.22a, the period of stratified flow is not obvious.

(3) Empirical correlation of pressure overshoot

In order to describe quantitatively the pressure overshoot, a new regression model is built up by analyzing the reason for producing the pressure overshoot.

The reason causing pressure overshoot is that the response speeds of pressure at different locations along the pipeline are different and there exist the acceleration effects of liquid slugs. The value of pressure overshoot is associated with the pressure drop for accelerating two-phase mixture. The equation for the acceleration pressure drop of two-phase flow may be a reference to establish a regression model for pressure overshoot prediction.

With the assumption that the liquid slug is free of gas bubble, the slug velocity and mass flux at initial steady state are U_{S1} and ρU_{S1} respectively, these at new steady state are U_{S2} and ρU_{S2} respectively. From momentum conservation, the acceleration pressure drop of liquid slug can be

written as follows (1992),

$$\Delta p_a = \rho U_{s2} U_{s2} - \rho U_{s1} U_{s1} = \rho (U_{s2}^2 - U_{s1}^2) \quad (26)$$

From Nicklin et al. (1962), the slug velocity is proportional to the homogeneous mixture velocity. Assume that the drift velocity V_∞ equals zero, considering the effects of gas compressibility, the lengths of liquid and gas slug and keeping meet the condition that the pressure overshoot must be zero if the change of gas flowrate is zero, the regression model can be gotten as follows,

$$\Delta p_{os} = a\rho(U_{m2}^2 - U_{m1}^2) \quad (27)$$

Where a is the regression coefficient.

Since the homogeneous mixture velocity U_m equals the sum of liquid superficial velocity V_{SL} and gas superficial velocity V_{SG} , and that the liquid superficial velocity is constant during the gas flowrate transient, Eq.(27) can be rewritten as follows:

$$\Delta p_{os} = a\rho[(V_{SG2} + V_{SL})^2 - (V_{SG1} + V_{SL})^2] \quad (28)$$

24 groups effective data were obtained in present experiment. Based on these data, a correlation for the pressure overshoot was finally obtained as follows,

$$\Delta p_{os} = a\rho[(V_{SG2} + V_{SL})^2 - (V_{SG1} + V_{SL})^2] \quad (28)$$

By T-test(test for averaged value analysis) and F-test(Fisher distribution function analysis test for root mean square deviation), Eq.(29) and the coefficient of equation is remarkable at remarkable level 0.0001.

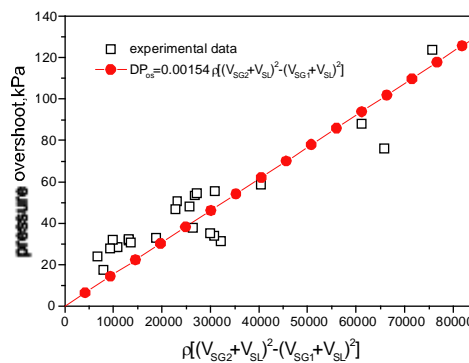


Fig. 25 The comparison between regression equation and experimental data

Fig.25 shows a comparison of the regression equation to the experimental data. From Eq.(29) and figure 25, it can be concluded that the value of pressure overshoot is directly proportional to a square of the difference of the homogeneous mixture velocities between in initial and final steady states. When the change of gas flowrate equals zero, the pressure overshoot is equal to zero

4.3.3 Liquid Flowrate Transients

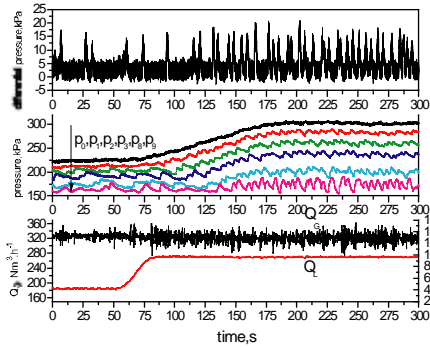


Fig. 26 “Up-liquid” transient

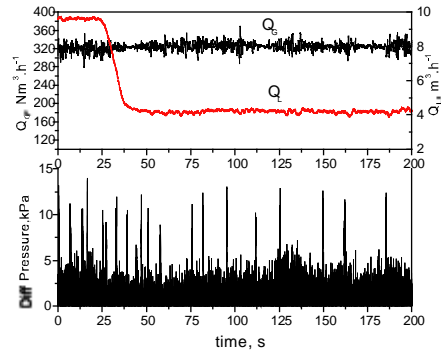


Fig. 27 “Down-liquid” transient

Fig. 26 shows the pressure and differential pressure profiles at the location of 245 m away from the entrance under “Up-liquid” transient. When the gas flowrate was kept constant, and liquid flowrate changed from a steady state to a new steady state. The flow regime of mixture is still slug flow during this transient.

Fig. 27 shows the differential pressure profile at the location of 245 m away from the entrance under “Down-liquid” transient.

During the liquid transients, the pressure changed smoothly to the new steady state value. The far the location of measuring point is from the entrance, the smaller the pressure change is. There was no pressure overshoot and no pressure undershoot in test section and no flow pattern transition occurred. Only the slug frequency appeared rapid change in this transient, because the slug frequency at a steady state depends strongly on the superficial liquid velocity. The new steady state was established quickly with two or three slugs to bridge the period. This suggests that the liquid level near the inlet responded quickly to the change of liquid flowrate, hence the slug formation at new steady state was established in a similar mechanism (1977).

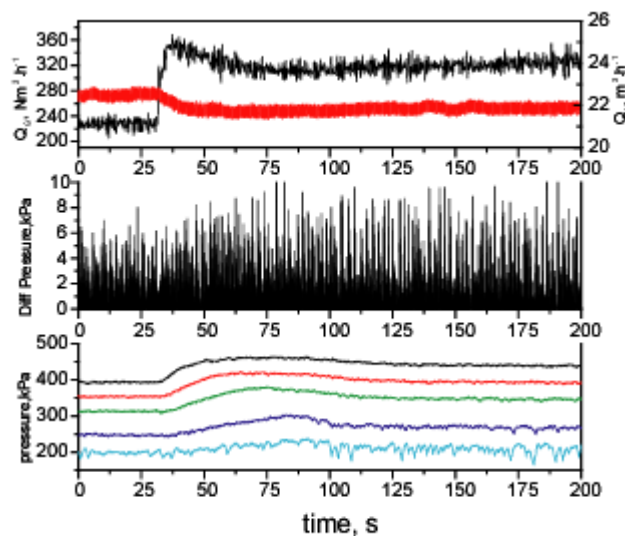


Fig. 28 Pressure and differential pressure changes of simultaneous change of gas and liquid flowrate

4.3.4 Simultaneous Change of Gas and Liquid Flowrate

In our experimental system, the change of gas flowrate had an effect on the liquid flowrate. The raising of the gas flowrate brought on a falling of liquid flowrate consequentially. In order to complete more tests in wider range, the gas regulator and liquid regulator were used to adjust the gas and liquid flowrate.

There are four cases of simultaneous transients, i.e., gas and liquid flowrates increase or decrease simultaneously, gas flowrate increases and liquid flowrate decreases, or otherwise. In our experiment, the third case is considered in which gas flowrate increases and liquid flowrate decreases. Fig. 28 shows the pressure and differential pressure profiles. There were a pressure overshoot and a decrease of slug frequency in this case. The feature of pressure overshoots and slug frequency change consisted with that of single-phase flowrate transient.

4.4 An Experimental Study of Severe Slugging in Offshore Pipeline/riser System

In the offshore oil and gas industry, liquid and gas are frequently transported in pipeline simultaneously. When the subsea pipeline is connected to the platform or onshore facility through a riser, there may be a special flow phenomenon, called severe slugging, occurring in the pipeline and riser configuration. Compared with normal hydrodynamic slug flow, the intermittent characteristics of severe slugging are stronger and regularly, such as the length of the liquid slug may be several times of the riser length and the pressure changes periodically and its fluctuation magnitude may be equal to the hydrostatic head of the riser full of liquid. Also, the liquid slug would be impelled with a higher velocity leaving the riser than the liquid velocity at the pipe inlet when the compressed gas in the pipeline expanded and flowed out of the riser exit. This phenomenon makes it very difficult to design the production facilities economically. Farghaly et al. (1987) reported that the liquid carry over of some separators at average production rate was only half of its nominated capacity. Also the operation of the downstream processing equipments would be very difficult when the severe slugging was occurring.

Some researchers have studied the severe slugging phenomenon in real field or laboratory. Yocum (1973) was the first to discuss the severe slugging encountered in several oil fields although he did not differentiate it from the conventional slug flow. Farghaly et al. (1987) also reported that the severe slugging was occurred and abnormal long liquid slugs were generated in offshore pipeline-riser systems. The impact of the severe slugging on the field operation was discussed comprehensively and a hydrodynamic model was presented. Whereas in most laboratory studies, small scale test rigs were used to study the severe slugging, such as reported by Schmidt et al. (1979,1985), Pots et al. (1987), Taitel et al. (1990), Tengedal (2002). In their test rigs, a buffer vessel before the liquid and gas mixer was used to simulate the extra length of the pipeline. In this paper, tests have been carried out in a large scale experimental facility that the length of the real pipeline was 127m and no buffer vessel was used. Therefore the effect of the severe slugging on the flow in the upstream pipeline could be studied rightly and vice versa.

4.4.1 Experimental Facility and Method

An experimental facility was designed and constructed for this study in the State Key Laboratory of Multiphase Flow at Xi'an Jiaotong University. A schematic diagram of the experimental facility is shown in Figure 29.

Clean and filtered tap water was driven by a multi-stage centrifugal pump and then measured by the electromagnetic flowmeters. Oil was supplied by a gear pump from an oil tank and then measured by a CMF050 or CMF200 Micro Motion mass flowmeter. Air was compressed by a screw compressor and flowed into a buffer vessel. Then the air was filtered and measured by an orifice plate or a digital vortex flowmeter before entering the mixer. A horizontal plate was fixed in the mixer pipe to get stratified flow regime at the initial part of the test section, as shown in Figure 4.1. The gas was injected above and the liquid below the segregation plate. After the mixer, liquid and air flowed into the test loop with stratified flow pattern.

The test loop was consisted of a 108m long horizontal section, a 19m long downward inclined section and a 16m high riser. The total length of the test loop is 143m. The downward section could be inclined between 0° and -5° from the horizontal and this section was connected to the riser at its lower end through a 30cm radius bend. In this study, the inclination angles were limited to 0° , -2° and -5° . Most segments of the test loop were consisted of stainless steel pipe, but several segments located at the horizontal, downward and vertical parts of the loop were made of PVC pipe and were clear and visualization. The inner diameter of the test loop was 50mm. At the end of the riser, the gas-liquid mixture was separated in a vertical separator which was operated under atmospheric condition. The air was vented to atmosphere and the liquid was returned to a liquid-liquid separator tank. Oil and water were separated and flowed back to the storage tanks and recirculated respectively.

In this study, air and water were used as the test fluids and the water was metered by the Micro Motion mass flowmeters for their high precision. The test rig was instrumented with many pressure and differential pressure transducers along the profile of the pipeline and riser. The liquid holdup near the outlet of the riser was measured by a gamma ray densitometer which was aligned horizontally through the vertical pipe center. A video camera was equipped to record the flow configuration in the horizontal, downward or vertical transparent pipe sections. The instruments also included a series of conductance probes mounted in the horizontal and downward PVC pipe sections to identify the liquid slugs and elongated bubbles. The temperatures of every phase before the mixer and the mixture at the outlet of the riser were measured by 4 thermocouples.

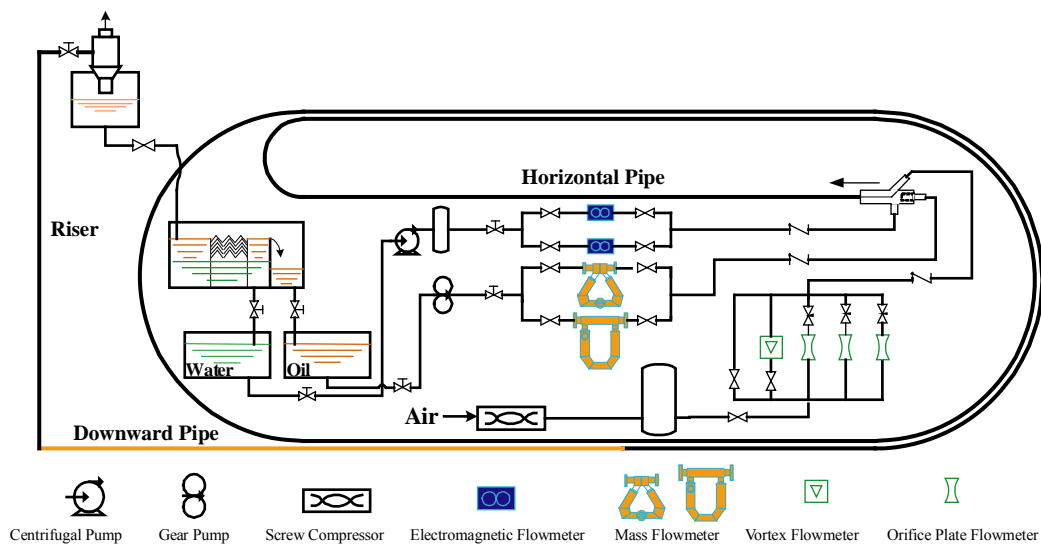


Fig. 29 Schematic of the test facility for severe slugging flow

The hardware of the data acquisition system consisted of a PC and a high speed multifunction board PCI-6071E made by National Instruments Inc. The data acquisition software, also called virtual instruments, was developed in the graphical programming system of LabVIEW6.0. The analog signals were acquired and stored into binary files and also could be displayed on the screen in waveform simultaneously. All the concerned signals were sampled at 500Hz.

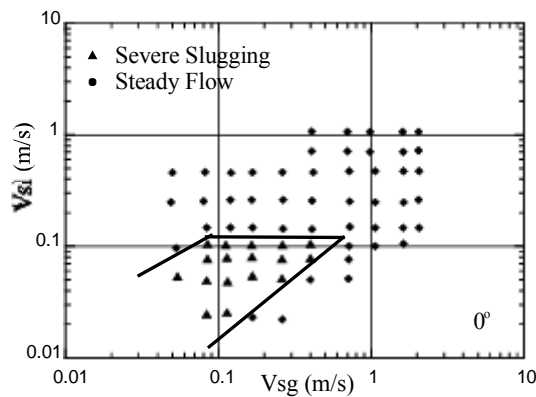
The liquid and air superficial velocities varied in the range of 0.01-2m/s and 0.01-5m/s respectively for this study. A 54600-Series oscilloscope, produced by Agilent Inc., was used to acquire and display two absolute pressure signals from the transducers located on the horizontal and vertical pipe sections. The pressure signals were analyzed and the cycle time could be acquired if there was cyclic process occurring in the facility. Moreover, determined from the real time information of the system pressures, if the constant operational conditions were reached, the acquisition program was run to collect

transient data for about several periods of severe slugging if this flow pattern was occurring in the test configuration. If the other stable flow patterns occurred, data was collected for 10 minutes. While the acquisition process was initiated, visual observations of the flow in the horizontal, downward inclined and vertical pipe sections were performed and the flow patterns were identified and recorded, together with the transition process of the flow patterns in a cycle time. Combined with the signals of pressure, differential pressure and liquid holdup displayed on the computer screen, it could be determined whether the flow in the pipeline-riser system was severe slugging or not.

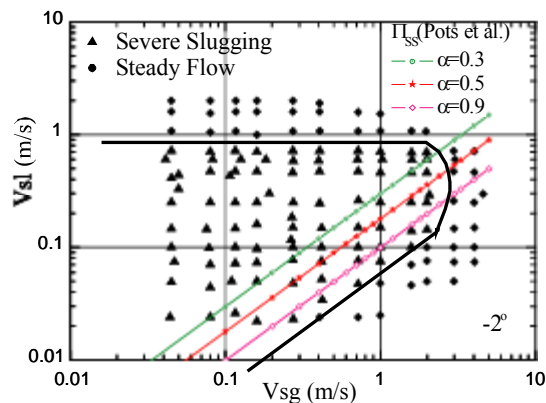
4.4.2 Results and Discussion

(1) Flow pattern map

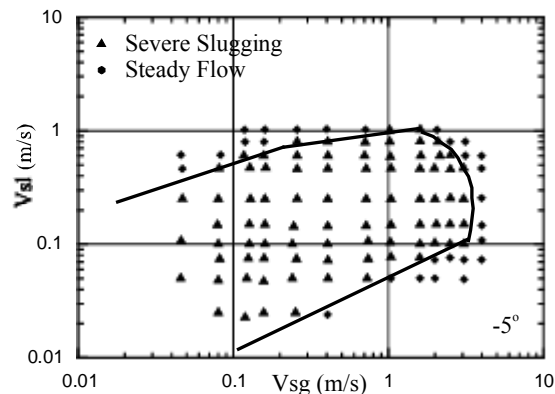
Figure 30 presents the experimental flow pattern maps that illustrate the occurring region of severe slugging as a function of the flow rates. The inclination angles of the downward pipe section of the three maps are 0° , -2° and -5° respectively. Note that the inlet gas liquid superficial velocity is normalized to the atmospheric condition. Except the severe slugging, the other flow patterns are classified as steady flow, which means that the flow patterns in the pipeline or the riser are fixed and do not change periodically, for example occurring of slug flow in pipeline and churn flow in the riser simultaneously.



(a) Downward pipe section angle of 0°



(b) Downward pipe section angle of -2°



(c) Downward pipe section angle of -5°

Fig. 30 Flow pattern map for various downward pipe section angles: 0° , -2° and -5° .

From these figures it can be seen that severe slugging is easier occurrence in the pipeline/riser system with a downward inclined pipe section before the riser. Compared with the maps of -2° and -5° inclination, Figure 30(a) shows that severe slugging only occurs in a very small area when the inclination of the downward pipe is 0° , i.e. the whole pipeline is horizontal. Also, the transition boundaries move down along both the liquid and the gas flow rates axes when the inclination angle is decreased to 0° , while the flow pattern in the pipeline is limited to stratified flow. However, when the inclination is increased to -2° or -5° , severe slugging is easily occurring in the system and there is no distinct difference between the flow pattern maps of the -2° and -5° inclination, as shown in Figure 30(b) and 30(c). Figure 31 shows all the experimental severe slugging cases of -2° inclination downward pipe section on the Mandhane horizontal flow pattern map. It can be seen that the flow pattern in the horizontal pipe section may be stratified flow, bubble flow or slug flow, which was also observed in the experiments. So severe slugging is easily encountered in field pipeline/riser system at low liquid and gas rates. From the experiments, it was observed that in most time of the severe slugging period the flow pattern in the downward pipe section was stratified flow though there might be several liquid slugs passing in the gas blowout process. Therefore this study agrees with the conclusion of Schmidt et al.(1985), they suggested that the stratified flow in the downward pipe section is a precondition for severe slugging. In their experiment the air accumulator before the mixer was used to simulate a long pipeline, however it was different from the real pipeline used in this study and the facility having the long pipeline can simulate the field offshore pipeline/riser system comprehensively. From the analysis, it can be concluded that stratified flow in the pipe section ahead of the riser, which is horizontal or downward, is the necessary condition for severe slugging occurrence. On the other hand, it was observed in the experiments that normal slug flow in the upstream horizontal pipe section and severe slugging in the whole system can coexist and both flow patterns are not mutually exclusive, which was also shown in Figure 30(b) and Figure31

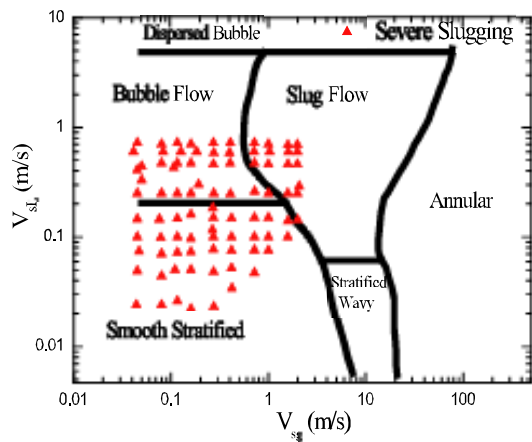


Fig. 31 Experimental severe slugging data of -2° downward pipe section shown on the flow pattern map for horizontal flow (Mandhane et al. 1974)

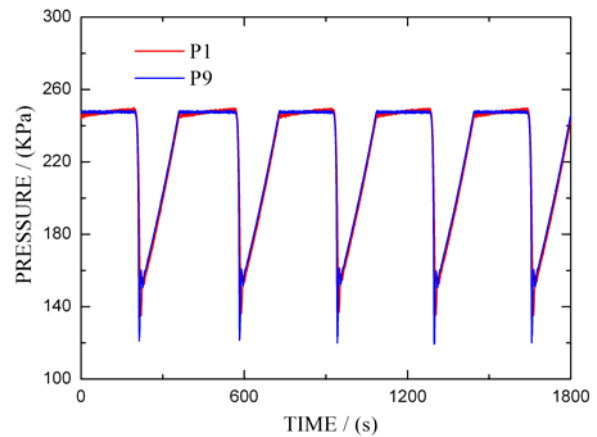


Fig. 32 Inlet pressure P1 and riser base pressure P9 vs. time, -2° inclination, $V_{sg}=0.12\text{m/s}$, $V_{sl}=0.15\text{m/s}$

Boe (1981) proposed a mathematical criterion to predict the severe slugging region. Later Pots et al. (1987) proposed a similar criterion considering that the rate of hydrostatic head buildup of the liquid in the riser caused by the growth of the slug must exceed the rate of gas pressure buildup in the pipeline. The ratio between the pressure buildup rates can be expressed as:

$$\Pi_{SS} = \frac{zRT/M}{gL_p\alpha} \frac{W_g}{W_L} \quad (30)$$

where W_g and W_L are gas and liquid mass flow rates respectively. α is the void fraction in the pipeline. L_p is the length of the pipeline. If $\Pi_{SS} < 1$, severe slugging could occur.

In Figure 28(b), three curves $\Pi_{SS}=1$ calculated for the test facility of this study are shown. The assumption value of the void fraction in the pipeline was 0.3, 0.5 and 0.9 respectively. It is expected that severe slugging would occur in the left region of these curves. It is shown that only the right curve with $\alpha = 0.9$ is close to the experimental boundary. Therefore this criterion does not predict the transition boundary of the flow patterns successfully.

(2) Pipeline pressure

Some experimental cases are presented in this paper and the flow characteristics of severe slugging are analyzed. The inclination angle of the downward section is limited to -2°.

Figure 32 shows the transient effect of the absolute pressures in the pipeline during several periods of the typical severe slugging, in which the liquid slug length is longer than the riser length. P1 is the inlet pressure of the system located 0.5m after the mixer and P9 is the pressure at the bottom of the riser. The air and liquid superficial velocities for this case were 0.12m/s and 0.15m/s respectively. From this figure it is shown that the pressures fluctuate periodically and regularly in severe slugging and have a period up to 360 seconds. The fluctuation magnitude of the inlet pressure P1 is 110KPa, while it is 124KPa for the riser bottom pressure P9. Also, it is found that both traces almost superpose each other in the cyclic process, though the distance is 127m between P1 and P9 transducers. Therefore the severe slugging has significant effect on the horizontal pipeline and the flow in that could not be treated separately from the whole system.

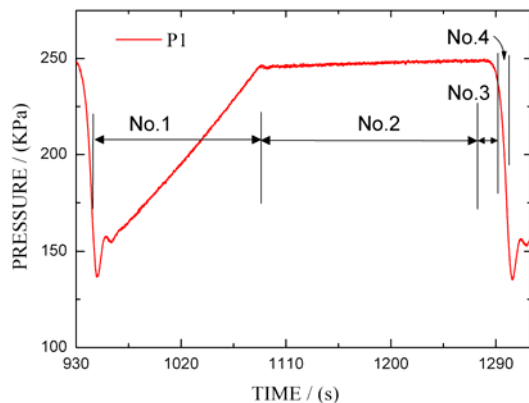


Fig. 33 Inlet pressure P1 vs. time in a severe slugging cycle, -2° inclination, $V_{sg}=0.12\text{m/s}$, $V_{sl}=0.15\text{m/s}$

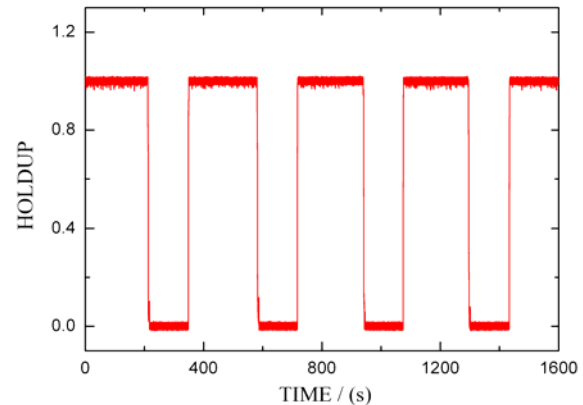


Fig. 34 Liquid holdup of riser vs. time, -2° inclination, $V_{sg}=0.12\text{m/s}$, $V_{sl}=0.15\text{m/s}$

Figure 33 shows the inlet pressure P1 in a severe slugging cycle time. As reported by Schmidt et al. (1985), the cycle of severe slugging can be divided into four stages:

- (1) Slug generation stage;
- (2) Slug production stage;
- (3) Bubble penetration stage;
- (4) Gas blowout stage.

From the experimental observation, it was found that during the gas blowout stage there were several liquid slugs passage in the downward pipe section in most cases and their lengths were longer than the length in normal slug flow. These liquid slugs were produced in the horizontal pipeline caused by the sudden expansion of the compressed gas for the pressure decrease and moved rapidly to the riser base and blocked the gas passage into the riser together with the liquid fallback in the vertical riser. After the blockage of the riser base, the following liquid slugs stopped moving in the downward pipe and filled it with the carrying liquid. The slug generation stage started again. Because of the slugging phenomenon occurring in the pipeline during gas blowout process, the length of liquid penetration into the downward pipeline in this study is longer than that only formed from the liquid fallback in the vertical riser pipe, such as reported by Schmidt (1979).

(3) Riser liquid holdup

Figure 34 presents the liquid holdup measured at the top of the riser from the gamma ray densitometer during severe slugging cycles. It is shown that the pipe area of the measured cross section had two conditions, “full” or “empty”, in most time and the transition time is very short. When the pipe was empty, it was during the slug generation stage and the liquid did not reach the top of the riser pipe. The holdup increased to unity when the liquid slug reached the top of the riser and the liquid began to flow into the separator. At the end of the bubble penetration stage and the beginning of the gas blowout stage, gas bubble reached the top of the riser pipe and gas flowed out violently. When the remaining liquid fell down the riser and blocked the bottom, the liquid holdup decreased sharply to zero and there was no fluids flow out of the riser. This process occurred in a very short time comparing with the whole severe slugging period, as shown in Figure 34. From the video recorded at the transparent vertical pipe section, it is found that the gas flowed in 16 seconds in a cycle. So it meant that the gas volume entering the pipeline in a severe slugging cycle time was compressed and released rapidly in a very short time.

(4) CLiquid slug length

In order to measure the liquid production, a special cylinder vessel was designed optimally and small liquid level changes could be indicated by the differential pressure transducer. A T-junction

equipped with an electromagnetic quick valve was used to switch the liquid stream into either the cylinder vessel or the liquid-liquid separator tank. The length of liquid slug flowing out of the riser could be calculated from the differential pressure between the bottom and the liquid level in the vessel.

Figure 35 shows the length of liquid slug produced in severe slugging vs. the liquid superficial velocity with -2° inclination of the downward pipe section. The riser length is also plotted in Figure 35. It is indicated that the liquid production in a severe slugging cycle time increases as the liquid flow rate increases when the gas flow rate is constant. However the liquid slug length decreases sharply as the gas flow rate increases. Therefore increasing the inlet gas flow rate is a feasible method to eliminate the severe slugging. From Figure 35, it is found that the maximum of the liquid slug length is about 7 times of the riser length.

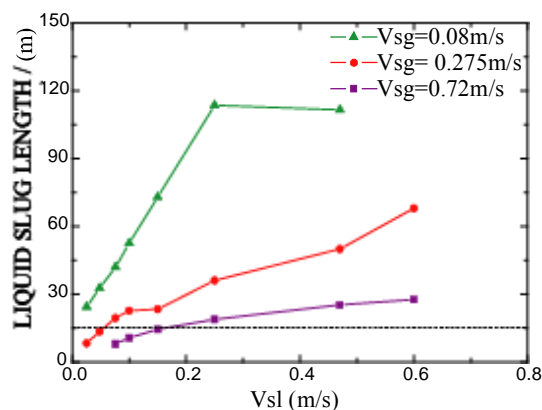


Fig. 35 Liquid slug length vs. liquid superficial velocity, -2° inclination

5. SUMMARY

5.1 Conclusions to the Flow Pattern Online Identification

The flow velocity of fluid and the oil fraction influence strongly the signal feature of pressure and differential pressure. The feature parameters for every flow pattern intersect seriously. To overcome the online recognition of industrial multiphase flow is very difficult only based on a single type of flow pattern information and processing method.

The recognition method based on feature space needs to meet two basic prerequisite. One is that the feature space about flow regime information should have sample set which can represent the feature of flow regime. The other is that the feature space should meet the principle of close cohesion for a certain flow regime, and far separation for different flow regimes.

The recognition rules for partial of flow pattern are proposed on the basis of decollating the feature space composed by the signal features of pressure and differential pressure. For every flow pattern feature the self-organization cluster algorithm is proposed to design the standard templates, which can be taken as the basis to recognize flow regime.

Based on the pressure and differential pressure signals, the multi-sensor data fusion method is proposed to realize the online recognition of multiphase flow regime, which can overcome the severe influence of flow velocity and the oil fraction of fluid on the recognition. The online recognition method is tested and confirmed in the practice, which has less than 10 percent measurement error. The method takes advantages of high confidence, good fault tolerance and less requirement over single sensor performance.

5.2 Conclusions to Slug Flow Tracking Model

Systematical experiments two-phase slug flow of air and water mixture were conducted on a 27.33m long horizontal pipe. The measurements of hydrodynamic parameters of slug flow evolution along the

pipe were completed by the differential pressure method. In this method Two close pressure transducers were used to measure the translational velocity of elongated bubble and the liquid slug length. From the experimental results, it was found that the averaged liquid slug lengths are not dependent on the mixture velocities, and the maximum and the averaged liquid slug length increase along the pipe.

A modified slug tracking model was presented in our laboratory which considered the affections of acceleration pressure drop and the wake effect. This model was programmed in C++ language with OOP technique. Compared with the data of observed liquid slugs, the model correctly predicted the length distributions with quite good agreement. Both the predicted and the measured liquid slug lengths followed a log-normal distribution. The model can predict the maximum slug lengths correctly. However the predicted averaged liquid slug lengths were longer than the experimental data, which was considered due to the separation effect of the elbow which decreased the length of the short slugs

5.3 Conclusions to the Experimental Study of the Flowrate Transients in Slug Flow

The results obtained in our laboratory demonstrate that the “Up-gas” transient would produce pressure overshoot. The magnitude of overshoot is related to the magnitude of change of gas flow rate and the distance away from the entrance. The further the distance is, the higher the magnitude of pressure overshoot. Near the exit, the pressure overshoot begins to decrease and is close to zero in the downstream slug catcher. Pressure waves exist in the pipeline, which spread from the entrance to the exit. The spreading speed of pressure wave decreases along the pipeline. At the same time, the increase of gas flow rate is often associated with the formation of larger slug.

The decrease of gas flow rate is associated with pressure undershoot and temporary stratified flow. The magnitude of pressure undershoots and period of stratified flow are sensitive to change of gas flow rate and the distance away from the entrance. With increasing the distance away from the entrance, the magnitude of pressure undershoots increase at first, then decrease linearly, but the period of stratified flow increase linearly.

Under liquid transients, the obvious feature is the change of liquid slug frequency. Based on the experimental results an empirical equation for the calculation of pressure overshoot was proposed in which the pressure overshoot was correlated with the acceleration pressure drop caused by the increase of gas flow rate.

5.4 Conclusions to Severe Slugging Flow

An experimental facility was designed and constructed to study the severe slugging in SKMFPE. A series of flow pattern maps were obtained and the effect of the inclination angle of the downward pipe was experimentally studied and analyzed. It was found that the stratified flow in the downward pipe is a precondition for the occurrence of severe slugging. However, the normal slug flow can be occurring in the horizontal pipe with the severe slugging occurring in the whole system. The hydrodynamic characteristics of severe slugging were reported, such as the pressure, the liquid holdup and the length of the liquid slug. Figure 35 shows that the liquid slug length decreases sharply as the gas flow rate increases at same liquid flow rate. Therefore, increasing the inlet gas superficial velocity is a feasible method to eliminate the severe slugging

REFERENCES

Acikgoz M, Franca F and Lahey R T Jr. (1992). An Experimental Study of Three-Phase Flow Regimes. *Int J of Multiphase Flow*. 18:327-336

Andritsos N. and T.J. Hanratty (1987). Interfacial instabilities for horizontal gas-liquid gas-liquid flows in pipelines. *Int.J. Multiphase flow*, .13(5):583-603.

- Bai B F. (1999). Flow Parameters Fluctuations and Online Automatic Identification of Flow Regime for Steam (Gas)-Water Two-Phase Flow. Ph.D Dissertation. Xi'an: Xi'an Jiaotong University, 1999: 3-15
- Bai B F, Guo L J, Zhao L. (2001). Development Of One-Line Identification Of Steam (Gas)-Liquid Two-Phase Flow Regimes. *Advances in Mechanics*, 31(3): 437-446
- Bai B F, Zhang S J, zhang X M , Zhao L., Guo L J. (2008). Online recognition of the multiphase flow regime, *Sci China Ser E-Tech Sci*, Aug. 2008, 51(8):1-9.
- Banjamin T.B. (1959). shearing flow over a wavy surface, *J.Fluid Mech.* Vol.6, pp.161-205.
- Barnea, D. (1991). On the effect of viscosity on stability of stratified gas-liquid flow-application to flow pattern transition at various pipe inclinations. *Chem. Engng. Sci.*, 46, 2123-2131.
- Barnea, D. & Taitel, Y. (1993). Kelvin-Helmholtz stability criteria for stratified flow: viscous versus non-viscous (inviscid) approaches, *Int. J. Multiphase Flow*, 19(4), 639-649.
- Barnea, D.A., Taitel, Y (1993). A model for slug length distribution in gas-liquid slug flow. *Int. J. Multiphase Flow*. 19, 829-838
- Barnea D., Taitel Y. (1994). Interfacial and structural stability of separated.flow, *Int. Multiphase Flow* 20 (Suppl.) 387-414.
- Bendiksen, K., Espedal, M. (1992). Onset of slugging in horizontal gas-liquid pipe flow, *Int. J. Multiphase Flow*, 18, 237-247.
- Bendiksen, K. H. et al. (1996). On the modeling of slug flow. *Chem. Eng. Comm.* V141-142, 71-102
- Boe, A. (1981). Severe slugging characteristics; Part 1: Flow regime for severe slugging; Par 2: Point model simulation study. Presented at Selected Topics in Two-Phase Flow, Trondheim, Norway, March 1981.
- Brauner N., Maron D.M. (1992). Stability analysis of stratified liquid-liquid flow, *Int. J. Multiphase Flow* 18, 103-121.
- Brill, J.P. et al. (1981). Analysis of two-phase tests in large-diameter flow lines in Prudhoe Bay Field. *SPEJ*, 363-378
- Cai, Y, Wambsganss M W, Jendrzeczyk J A. (1996). Application of Chaos Theory in Identification of Two-phase Flow Patterns and Transitions in a Small, Horizontal, Rectangular Channel. *ASME J Fluid Engineering*, 118: 383-390
- Caussade, B., Fabre, J., The'ron, B. (1987). Unsteady gas-liquid flow in horizontal pipes, European Two-Phase Flow Group Meeting, Trondheim, Norway
- Chu, K.J. and Dukler, A.E. (1974). Statistical characteristics of thin, wavy films: II Studies of the substrater and its wave structure. *AIChE J.* 20, 695-706.
- Chu, K.J. and Dukler, A.E. (1975). Statistical characteristics of thin, wavy films: III Structure of the large waves and their resistance to gas flow. *AIChE J.* 21, 583-593.
- Cook, M.&Behnia, M. (2000). Slug length prediction in near horizontal gas-liquid intermittent flow.

Chem. Eng. Sci. 55, 2009-2018

Crowley C.J., Wallis G.B., Barry J.J. (1992). Validation of a one-dimensional wave model for the stratified to slug flow regime transition, with consequences for wave growth and slug frequency, *Int. J. Multiphase Flow* 18 (2) 249–271.

Dukler, A. E., Hubbard, M. G (1975). A model for gas-liquid slug flow in horizontal and near horizontal tubes. *Ind. Engng Chem. Fundam.* 14, 337-347

Farghaly, M.A. (1987). Study of severe slugging in real offshore pipeline riser-pipe system. SPE 15726, Presented at SPE Middle East Oil Show, Manama, Bahrain, March, 1987.

Funada, T., Joseph, D.D. (2001). Viscous potential flow analysis of Kelvin–Helmholtz instability in a channel. *Int. J Multiphase Flow* 28(9), 263–283.

Giovine D. (1991). Stability of liquid flow down an inclined tube, *Int. J. Multiphase Flow* 17,485–496.

Guo L,J, Li G,J, Chen X,J (2002). A linear and non-linear analysis on interfacial instability of gas-liquid two-phase flow through a circular pipe.*Int,J. Heat and Mass transfer*,45,1525-1534.

Guo L J. (2002). Two-phase and Multi-phase Flow Dynamics. Xi'an: Xi'an Jiaotong University Press, 2002

Guo Liejin, Gu Hanyang, Wang Xin, Chen Xuejun (2005). Interfacial waves and slug flow in pipeline, in Proceeding of 5th int. symp on multiphase flow, heat mass transfer and energy conversion, Xi'an, 2005.

Hall, David L. (2001). Handbook of Multisensor Data Fusion. New York: CRC Press, 2001

Hanratty, T.J., Engen, J.M. (1961). Interaction between a turbulent air steam and a moving water surface, *AICHE J.*7, pp488-497

He Limin (2002). An investigation of the characteristics of oil-gas two-phase slug flow in horizontal and near horizontal pipes. Ph.D. Dissertation. Xi'an Jiaotong Univ.

Huang R, Zhong B L. (1991). Monitor and Failure Diagnosis during Machine Manufacture. Xi'an: Xi'an Jiaotong University Press, 1991: 48-70

Hubbard M G, Dukler A E. (1966). The Characterization of Flow Regimes for Horizontal Two-phase Flow. In: M.A.Saad & J.A.Moller eds. Proc. of the 1966 Heat Transfer and Fluid Mechanics Institute, Stanford University Press, 100-121

Jeffreys, H. (1925). On the formation of water waves by wind, *Proc.R.Soc. A* , 107,189.

Jurman L.A., M.J. (1989) Study of waves on thin liquid film sheared by turbulent gas flows, *Phys. Fluids A* 1,522–536.

King, M. J. S., Hale, C. P., Mendes-Tatsis, M. A., Hewitt, G. F. (1996). An experimental investigation of the effect of flowrate transients within the slug flow regime in horizontal pipes, 7th International Conference on Pressure Surges and Fluid Transients in pipelines and Open Channels, Harrogate, UK.

King, M. J. S., Hale, C. P., Lawrence, C. J., Hewitt, G. F. (1998). Characteristics of flowrate transients in slug flow, *Int J Multiphase Flow*,24, 825-854.

- Kohonen T. (1990). The Self-Organizing Map. *Proceedings of the IEEE*. 1990, 178 (9): 1464-1480
- Langford H M, Beasley D E, Ochterbeck J M. (1998). Chaos Analysis of Pressure Signals in Upward Air-water Flows. *Third International Conference on Multiphase Flow, ICMF'98, Lyon, France, June 8-14*
- Lay. C.E. and Dukler A.E.(1994) Flooding in vertical tubes-II A film model for entry region flooding. *Int.J. Multiphase flow*, Vol.20, No.2, pp.235-247.
- Li, G.J. (1996). Ph. D Thesis School of Energy and power Engineering Xi'an jiaotong University, Xi'an (1996)
- Li H. (2002). Application Of Wavelet Multi-Resolution Analysis To Pressure Fluctuations Of Gas-Solid Two-Phase Flow In A Horizontal Pipe. *Powder Technology*, 2002, 125:61-73.
- Lin P.Y., Hanratty T.J. (1986). Prediction of the initiation of slugs with linear stability theory, *Int. J. Multiphase Flow* 12,79-98.
- Lin, Zonghu, (1992). Characteristics of gas-liquid two-phase flow in pipelines and their engineering application, Xi'an Jiaotong University Press, 57-59.
- Mahvash A, Ross A. (2008). Two-phase Flow Pattern Identification Using Continuous Hidden Markov Model. *Int J of Multiphase Flow*, 34 (1): 303-311
- Mandhane J M, Gregory G A and Aziz K. A. (1974). Flow Pattern Map for Gas-Liquid Flow in Horizontal Pipes. *Int J of Multiphase Flow*, 1: 537-553
- Matsui G. (1986). Automatic Identification of Flow Regimes in Vertical Two-phase Flow Using Differential Pressure Fluctuations. *Nuclear Engineering and Design*, 95:221-231
- Mi Y, Ishii M, Tsoukalas L H. (1998). Vertical Two-Phase Flow Identification Using Advanced Instrumentation and Neural Networks. *Nuclear Engineering and Design*, 184:409-420
- Miles J.W. (1959). On the generation of surface wave by shear flows. *J.Fluid Mech.* Vol.3, pp.185-204.
- Minami, K. (1991). Tansient flow and pigging dynamics in two-phase pipelines, PhD Thesis, University of Tulsa, Tulsa, OK, USA.
- Moissis, R., Griffith, P. (1962). Entrance effects in a two-phase slug flow. *J. Heat Transfer*. 84, 29-39
- Monji H, Matsui G. (1998). Flow Pattern Identification of Gas-liquid Two-phase Flow Using a Neural Network. *Third International Conference on Multiphase Flow, ICMF'98, Lyon, France, June 8-12,*
- Nicklin, D. J., Wilkes, J. O., Davidson, J. F. (1962). Two-phase flow in vertical tubes, *Tans Inst Chem Eng*, 40, 61-68.
- Nydal, O. J. et al.(1992). Statistical characterization of slug flow in horizontal pipes, *Int. J. Multiphase Flow*. 18, 439-453
- Nydal, O. J. et al. (1996). Dynamic slug tracking simulations for gas-liquid flow in pipelines. *Chem. Eng. Comm.* V141-142, 13-39

Pots, B.M., Bromilow, I.G., Konijn, M.J. (1987). Severe slug flow in offshore flowline/riser systems. Soc. Pet. Eng. J., SPE13723, , 319-324.

Sakaguchi, T., Akagawa, K., Hamaguchi, H., Ashiwake, N. (1973). Transient behaviour of air-water two-phase flow in a horizontal tube, Winter Annual Meeting of Heat Transfer Division ASME, Detroit, MI, USA, November.

Samways A L, Bradbury L J S, Bruun H H.(1997). Pressure Measurements and Convection Velocity Evaluations in Two-Phase Flow. Int J of Multiphase Flow, 23(6):1007-1029

Schmidt, Z., Brill, L.P., Beggs, D. (1979). Experimental study of severe slugging in a two-phase flow pipeline-riser-pipe system. SPE8306. Presented at SPE Annual Technical Conference and Exhibition, Las Vegas Nevada.

Schmidt, Z., Doty, D.R., Dutta Roy, K. (1985) Severe slugging in offshore pipeline riser-pipe system. Soc. Pet. Eng. J., SPE12334, 27-38.

Sharma, Y. (1985). Modeling transient two-phase slug flow. Ph.D. dissertation. Univ. Tulsa.
Shi J. and Kocamustafaogullari, G., 1994, Interfacial measurements in horizontal stratified flow patterns, Nuclear Engineering and Design, 149, 81

Taitel, Y. and Dukler, A.E. (1976). A model for predicting flow regime transitions in horizontal and near horizontal gas-liquid flow. AIChE J. 22, 47-55.

Taitel, Y., Lee, N., Duckler, A. E. (1978). A model for slug flow frequency during gas-liquid flow in horizontal and near horizontal pipes, Int J Multiphase Flow, 3, 585-596.

Taitel Y, Vierkandt, S, Shoham O, Brill JP. (1990). Severe Slugging in a riser system: Experiments and Modeling Int. J. Multiphase Flow. 16(1): 57-68.

Taitel, Y. et al. (1998). Effect of gas compressibility on a slug tracking model. Chem. Eng. Sci. 53, 2089-2097

Taitel, Y. & Barnea, D. (1999). Slug tracking in hilly terrain pipelines. SPE Ann. Tech. Conf. Exhib. Prod. Oper. and Eng. Houston, 321-330

Takahama, H. and Kato, S. (1980). Longitudinal flow characteristics of vertical falling liquid films without concurrent gas flow. Int. J. Multiphase Flow 6, 203-215.

Tengesdal, J.O. (2002). Investigation of self-lifting concept for severe slugging elimination in deep-water pipeline/riser systems. Ph.D. Thesis, Pennsylvania State University.

Tutu N K. (1984). Pressure Drop Fluctuations and Bubble-Slug Transition in a Vertical Two-phase Air-water Flow. Int J of Multiphase Flow, 10 (2):211-216

van Hout et al. (2001). Evolution of statistical parameters of gas-liquid slug flow along vertical pipes. Int. J. Multiphase Flow. 27, 1579-1602

Wambsganss M W, Jendrzeczyk J A, France D M. (1991). Two-phase Flow Patterns and Transitions in a small Horizontal, Rectangular Channel. Int J of Multiphase Flow, 17 (3):327-342

Woods, B.D., Hanratty, T.J. (1996). "Relation of slug stability to shedding rate", Int. J. Multiphase Flow, 22, 809~828.

Wu Haojiang, Zhou Fangde, Wu Yuyuan. (2001). Intelligent Identification System of Flow Regime of Oil-Gas-Water Multiphase Flow. *Int J of Multiphase Flow*, 27: 459-475

Yang G, Wang Y T, Lu Z X, and et al. (2005). Application of Multi-sensor Data Fusion in Multiphase Flow Parameter Measurement. *Instrument Technique and Sensor*, No.11: 51-53

Yocum, B. T. (1973). Offshore riser slug flow avoidance: mathematical models for design and optimization. SPE4312, Presented at SPE European Meeting, London, April, 1973.

Zheng, G.H. et al. (1994). Slug flow behavior in a hilly terrain pipeline. *Int. J. Multiphase Flow*. 20, 63-79